

# **pH RESPONSIVE POLYSACCHARIDE VESICLES FOR DRUG DELIVERY**

Thesis submitted towards the partial fulfillment of  
BS-MS dual degree program



By

**THAMEEZ MOHAMMED K Y**

**20101038**

Under the guidance of

**Dr. M. JAYAKANNAN**

Associate Professor

Department of Chemistry

Indian Institute of Science Education and Research (IISER-Pune)

## CERTIFICATE

This is to certify that this dissertation entitled "**pH responsive polysaccharide vesicles for drug delivery**" towards the partial fulfilment of the BS-MS dual degree program at the Indian Institute of Science Education and Research, Pune represents original research carried out by Thameez Mohammed K Y, IISER Pune under the supervision of **Dr. M. Jayakannan**, Associate Professor, Chemistry department during the academic year 2014-2015.

Date: 25-Mar-15

Place: Pune

  
Signature  
25/3/2015

## DECLARATION

I hereby declare that the matter embodied in the report entitled "**pH responsive polysaccharide vesicles for drug delivery**" are the results of the investigations carried out by me at the Department of Chemistry, Indian Institute of Science Education and Research, Pune, under the supervision of Dr. M. Jayakannan and the same has not been submitted elsewhere for any other degree.

Date: 25-Mar-15

Place: Pune



Signature

## ACKNOWLEDGEMENT

It is my immense pleasure to thank those who made this thesis possible. First and foremost, I would like to thank my advisor **Dr. M. Jayakannan** for his immense support and guidance. I feel privileged to be among his students. He celebrates research in the truest sense of the term. I would also like to thank him for providing us with such an excellent opportunity, and also for his encouragement throughout entire duration of the project. Despite his busy schedule, he always found time to discuss with us and guide us throughout the project. His guidance has been an extraordinary learning experience.

I would like to express my sincere gratitude to Prof. K. N. Ganesh, director IISER-Pune for the state-of-the-art amenities and instrumentation at IISER,Pune.

I would like to thank **Pramod P.S, Smita Kashyap and Nilesh Deshpande** who mentored me during the course of the project. They provided me with the insight, constant help throughout the project and answered all my questions patiently.

I thank all my lab mates **Ananthraj, Bapu, Narasimha, Rajendra, Sonashree, Bhagyashree, Mehak and Maitreyee** for making the memories in lab fond and special. This place has left a lasting impression on me. This has been undoubtedly the best environment I have studied in and above people were responsible for it.

Last but not the least, I owe my deep sense of gratitude to my family and friends as they stood by me during the good and hard times.

~Thameez

## CONTENTS

<b>1. Abstract</b>	<b>6</b>
<b>2. Introduction</b>	<b>7</b>
2.1 Introduction	7
2.2 Polymers as drug carriers and EPR effect	8
2.3 Dextran based drug delivery carriers	10
2.4 pH responsive polymer scaffolds	13
2.5 Aim of the thesis	15
<b>3. Materials and Methods</b>	<b>17</b>
3.1 Materials	17
3.2 Methods	17
3.3 General procedures	18
<b>4. Results and Discussions</b>	<b>23</b>
4.1 Synthesis of Dex-CHO-x and characterization	23
4.2 Synthesis of Dex-IM derivatives	26
4.3 Self-assembly of Dex-IM derivatives	28
4.4 Encapsulation studies	31
4.5 In vitro release studies	36
<b>5. Conclusion</b>	<b>38</b>
<b>6. References</b>	<b>39</b>

## ABSTRACT

This thesis emphasizes on the design and synthesis of pH responsive amphiphiles based on biodegradable dextran as hydrophilic segment and different hydrophobic units. In this work, the role of hydrophobic part in the molecular self-assembly of amphiphiles into vesicles were studied in detail by using linear, branched and aromatic long chains as hydrophobic segments. The newly synthesized amphiphiles were characterized by NMR and FT-IR technique. Self-assembly of these amphiphiles in aqueous medium was investigated using FE-SEM and dynamic light scattering (DLS) techniques. From the self-assembly studies, it was inferred that only the amphiphile having pentadecylphenol (PDP) as a pendant group (i.e. Dex-PDP-IM) self-organized to form vesicles of 190 nm diameter. While, other amphiphilic dextran derivatives self-assembled to form nanoparticles of 140-170 nm. Further, the loading efficiency of these scaffolds were evaluated by using three different dyes; Rhodamine B (hydrophilic dye), Nile Red and Pyrene (hydrophobic dyes). Dex-PDP-IM based vesicle successfully encapsulated both hydrophilic and hydrophobic dyes independently. Additionally, these dextran vesicles exhibited dual drug loading phenomena. In other words, simultaneously both Rh B and pyrene were efficiently loaded in to the dextran based vesicular scaffold. Pyrene gets localized in the hydrophobic layer, while Rh B in the inner aqueous interior of the vesicle. The release kinetics of Rh B encapsulated Dex-PDP-IM was investigated at pH 7.4 (physiological pH), 5.5 (endosomal pH) and 2 (extreme acidic condition). Acidic pH was employed as the stimuli since the nanoscaffold is having an imine linkage, which is acid labile. At physiological pH, around 45-50% of the dye was retained in the vesicle. On the other hand, at lower pH i.e. 5.5 almost 80% of the dye gets released due to hydrolysis of imine linkage and at pH = 2, 100% of the dye leaches out from the vesicle. Thus the tailor made Dex-PDP-IM is a highly potent nanocarrier to delivering both hydrophobic as well as hydrophilic anticancer drug to the targeted tumor tissues.

## 1.1. INTRODUCTION

The physiological events such as proliferation, differentiation, apoptosis and cell arrest modulates the metabolic equilibrium and functionality of all tissues<sup>1</sup>. A condition where any dysregulation to these sequential events can lead to change in the ratio between cell differentiation, cell proliferation and cell death, results in number of dysregulated cells termed as cancer<sup>1</sup>. Cancer is one of the deadliest disease that we face in the current century. Several anti-cancer drugs have been formulated till date. However, majority of anti-cancer drugs are hydrophobic in nature. Poor solubility of the most of the anticancer drugs leading to low drug bioavailability and reduced therapeutic efficacy is one of the major problem associated with cancer therapy<sup>2</sup>. Moreover, through hydrophobic interactions these drugs interacts with plasma proteins which in turn provokes RES (reticulo-endothelial system), resulting in opsonisation by macrophages<sup>3</sup>. These features make the design of drugs difficult. Thus, delivering of drug to the target site without affecting its pharmacophore is of utmost importance.

In order to overcome the short comings of conventional drug therapy the concept of drug delivery was introduced. Drug delivery is the method of administering a pharmaceutical compound in humans or animals in order to achieve a therapeutic effect<sup>4</sup>. In general, drug molecules show a therapeutic window where drug plasma level is the key factor in determining the toxicity as well as efficiency of the drug (see Fig 1.1)<sup>5</sup>. Using conventional delivery systems due to its frequent dosage of drugs, it is not feasible to administer drug in therapeutic window range. Thus, to maximize the therapeutic efficacy of the anti-cancer drugs several controlled release devices were fabricated. Apart from improving drug efficacy, controlled release system offers several other advantages over conventional systems (capsules, ointment, injections etc.) such as increased drug bioavailability, reduced toxicity and improved patient compliance<sup>5</sup>. In other words, controlled release systems increase the efficacy of drug by delivering the drug over an extended duration or at a specific time during treatment assuring very small fluctuations in the drug concentration (Fig 1.1). Also, one of the major goals in therapeutic and diagnostic applications is the need of retaining the drug in the blood stream which is often hampered by the short in vivo half-life of the administered drugs<sup>6</sup>.

Since the controlled release devices minimize the interaction of the encapsulated drug with the blood components, the renal clearance of the drugs is reduced, thereby increasing the blood half-life of the drugs. Thus, controlled release systems are widely explored in cancer therapy owing to low water solubility and poor selectivity of anticancer drugs.

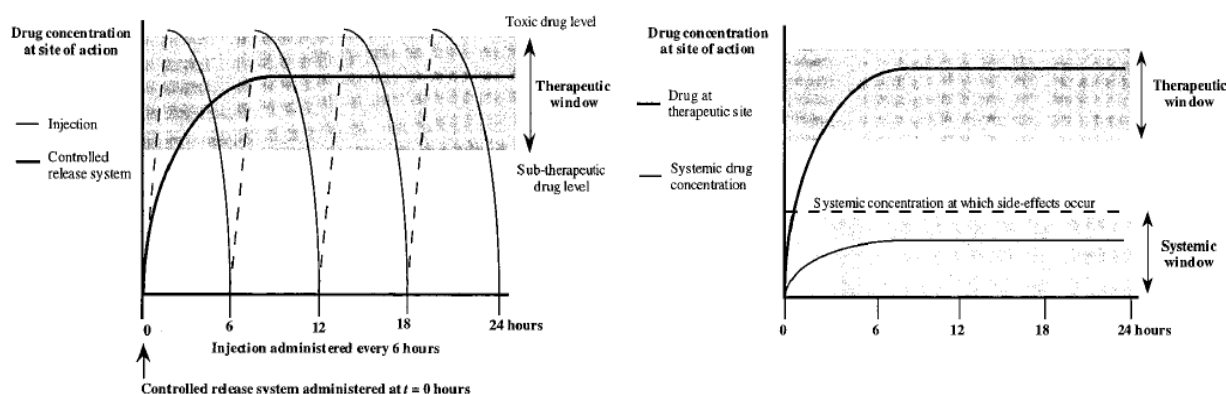


**Fig 1.1.** Comparison of therapeutic actions of conventional injection (thin line) and controlled release system (bold line). (Adopted from *Uhrich, K.E.; Canizzaro S.M.; Langer, R.; Shakesheff, K.M. Chem. Rev., 1999, 99, 3181*)

## 1.2 POLYMERS AS DRUG CARRIERS AND EPR EFFECT

It is well known that polymer, lipid or surfactant can encapsulate a pharmaceutical agent and release it in a controlled fashion at the desired site. The growing interest in polymer chemistry combined with biologically compatible molecules has led to the fabrication of variety of innovative polymeric drug delivery systems that are suitable for in vivo studies<sup>7</sup>. Prolonged circulation, controlled release rate and localized delivery with ease of administration are the desirable features of a drug delivery system. So, considerable efforts have been made in investigating systems such as polymeric microspheres, micelles, vesicles and liposomes<sup>8</sup>. These scaffolds offer additional privileges like high loading capacity, required stability in bloodstream, selective targeting and long circulating properties. In order to achieve above mentioned properties of the drug, numerous biodegradable polymers have been widely explored due to their unique advantages like lesser side effects, prolonged bioactivity, decreased administration frequency, thereby facilitating patient compliance<sup>9</sup>.



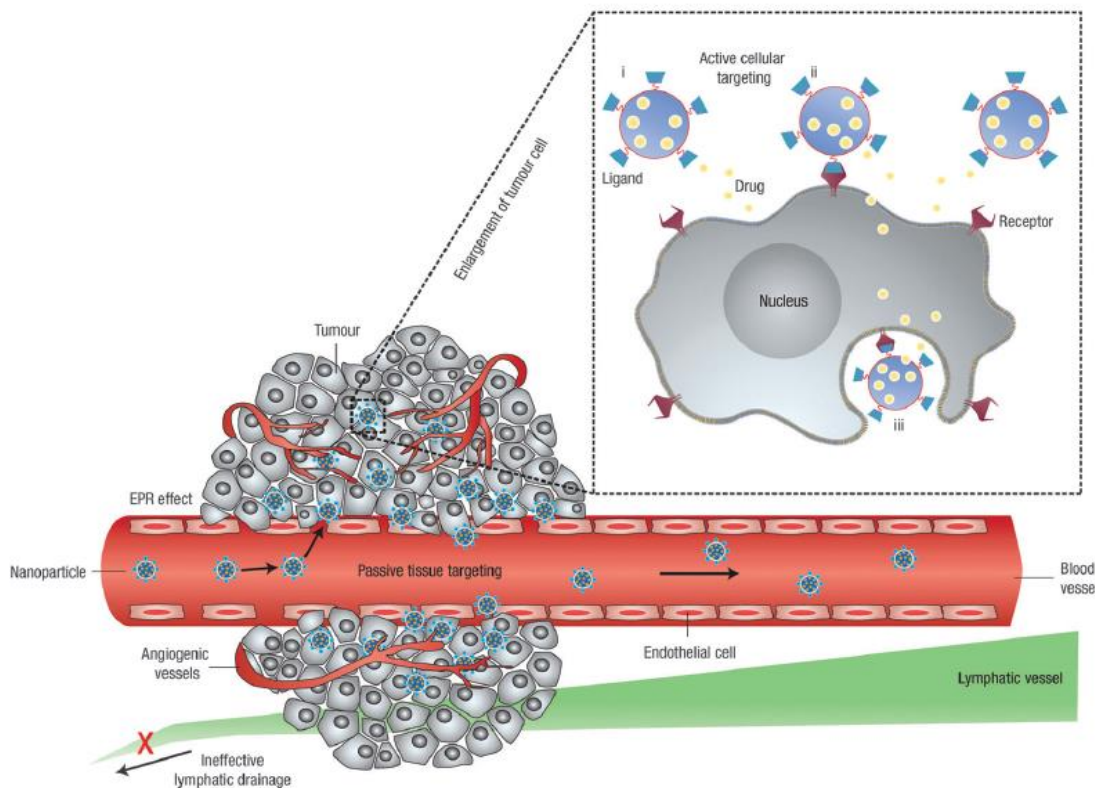


**Fig.1.2** Illustrates the passive (extravasation of nanoparticle through EPR effect) and active (functionalizing surface of nanoparticles with targeting ligands) tumor targeting using EPR effect. (Adopted from Nat Rev Cancer 2006 Sep; 6(9): 688-701.)

These macromolecule based drug carriers have an advantage of undergoing preferential accumulation in tumor tissue via EPR (enhanced permeability and retention) effect. In 1986, Matsumura and Maeda first reported about EPR effect<sup>10</sup> and later it was validated by Maeda *et al*<sup>11-14</sup>. Their studies showed that most of the solid tumors are usually associated with defective and leaky architecture of blood vessels. Also, extensive amounts of various vascular permeability factors are produced at the tumor site. As a result, vascular permeability of tumor blood vessels gets enhanced. This unique anatomical-pathophysiological feature of tumor blood vessels helps in facilitating macromolecules larger than 40 kDa to selectively leak out from tumor blood vessels and accumulate into tumor tissues. On the other hand, this EPR driven accumulation of drug does not occur in normal cells. Thus EPR effect is considered to be a landmark principle in anticancer drug design and tumor targeting chemotherapy<sup>11</sup>.

With aim of achieving higher accumulation and release of the chemotherapeutic agent at the desired site variety of synthetic as well as natural polymers has been

extensively used for drug delivery applications. Among synthetic polymers poly (lactic acid)-poly ethylene glycol block (PLA-b-PEG), poly (L-lactide)-poly ethylene oxide (PLL-b-PEO) and polystyrene-poly ethylene oxide (PS-b-PEO) block were commonly used for drug delivery applications<sup>15,16</sup>. However, one of the major challenges associated with synthetic polymers are their biodegradability and biocompatibility. Thus, naturally available polymers like polysaccharides which impart low toxicity due to its intrinsic nature of being biocompatible and biodegradable are extensively explored<sup>17,18</sup>. Of various polysaccharides known chitosan, alginate, hyaluronan, dextran, heparin pullulan and cyclodextrins are extensively used in drug delivery research. Among all, dextran bears several advantages such as high water solubility, biocompatibility, biodegradability, lack of nonspecific cell binding and resistance towards protein adsorption<sup>19</sup>. Additionally, the polymer consists of several reactive sites such as free hydroxyl group for further functionalization<sup>17</sup>.

### **1.3 DEXTRAN BASED DRUG DELIVERY CARRIERS**

Dextran is a branched polysaccharide made of glucose units. It consists of straight chain  $\alpha$  (1-6) glycosidic linkages and branches from  $\alpha$  (1-3) linkages. Dextran has been used clinically for last six decades as antithrombotic agents, anticoagulant agent etc. Since dextran is completely hydrophilic in nature it does not exhibit self-assembly property in aqueous medium. Therefore, to impart amphiphilicity to the polymer, conjugation of hydrophobic units to the polymer backbone is essential which in turn will result in formation of self-assembled structures. Recently, Lecommandoux and coworkers have shown the grafting of polystyrene of various molecular weights on the dextran backbone<sup>20</sup>. The degree of substitution was fixed to be 40 whereas length of polystyrene units was varied. They found that depending on the number of repeating units of styrene as well as solvent the copolymer self-assembled into either micelle or vesicle. Similarly, Yu-Ling Li *et al* reported a reversibly stabilized multifunctional dextran nanoparticles for the delivery of anticancer drug doxorubicin to the cancer cells<sup>21</sup>. They synthesized lipoic acid conjugated dextran copolymer with various degree of substitution. It was further cross-linked with dithiothreitol (DTT) to obtain crosslinked dextran nanoparticles, which successfully encapsulated Dox in its inner core with 84%

of drug loading efficiency. Over expressed glutathione present in the cancer cell lines with the capability of cleaving the disulfide linkage leads to release of drug from the nanoparticles in the intracellular compartment. (Fig.1.3). Further, the cytotoxic studies for the DOX loaded dextran nanoparticles showed 70% cell death in 48 h. Thus it indicates, that dextran based nano-scaffolds were efficient in delivering the drug at the target site.

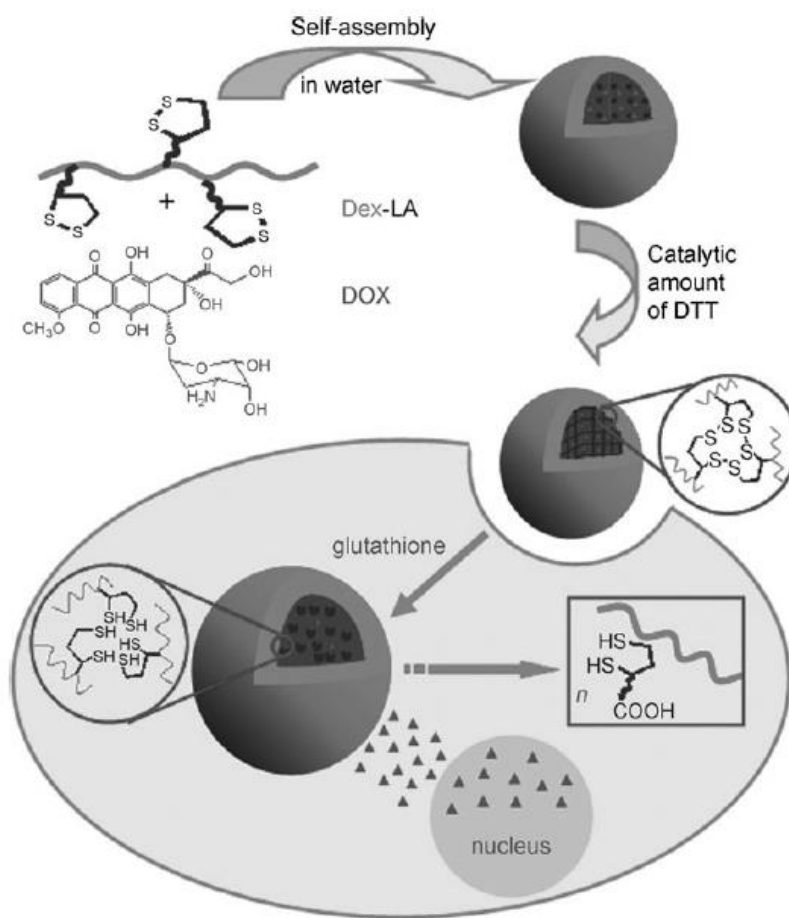


**Fig.1.3** shows the schematic of dextran crosslinked nanoparticle and their reductive triggered release of DOX by glutathione. (Adopted from *Angew. Chem. Int. Ed.* 2009, 48, 9914 –9918)

Upon comparing various self-assembled structure such as micelles, hydrogels, and vesicles etc., it has been observed that vesicles possess various advantages owing to their efficient cell penetrating ability, resistance against plasma proteins, longer circulation time and so on. The work done by Pramod *et al*, from our research group about dextran based drug delivery vehicles are worth mentioning. Wherein dextran vesicular nanoscaffolds were synthesized based on polysaccharide and

pentadecylphenol (PDP) as hydrophobic unit obtained from renewable source cashew nut shell liquid<sup>22</sup>. With 5% degree of substitution of 3-pentadecylphenol to the dextran backbone connected via an ester linkage leads to the formation of vesicular assembly in water. The resulting polymersome was capable of encapsulating two different moieties; such as hydrophobic camptothecin in the outer hydrophobic layer of vesicles and hydrophilic dye like rhodamine B (Rh B) in the inner core (Fig.1.4 a). Moreover, retention of active form of camptothecin (lactone form) inside the vesicular assembly was confirmed by HPLC technique. Since esterase enzymes are over-expressed in cancer cells, the in vitro release studies were done under physiological conditions using esterase enzyme which can destroy the vesicular assembly by cleaving the ester bond that connects PDP with dextran thereby leading to controlled release of drug to occur. 40% of the hydrophilic dye Rh B leached out in absence of esterase enzyme, which was further increased to 75% in presence of enzyme due to the disassembly of vesicular structures. Similarly in case of hydrophobic drug CPT, intrinsic leaching was found to be 60% and upon esterase activity almost 100% of the drug oozes out over a period of 48 hours. Cytotoxicity studies showed that dextran vesicular scaffolds were nontoxic to living cells and in the case of CPT loaded scaffold 2.5 fold increase in killing was found than normal CPT alone. Since the polymersomes were capable of encapsulating hydrophobic and hydrophilic drug independently as well as showing better killing effect as compare to free drug, dual drug encapsulation and release can lead to further enhancement in the drug efficacy for cancer treatment.

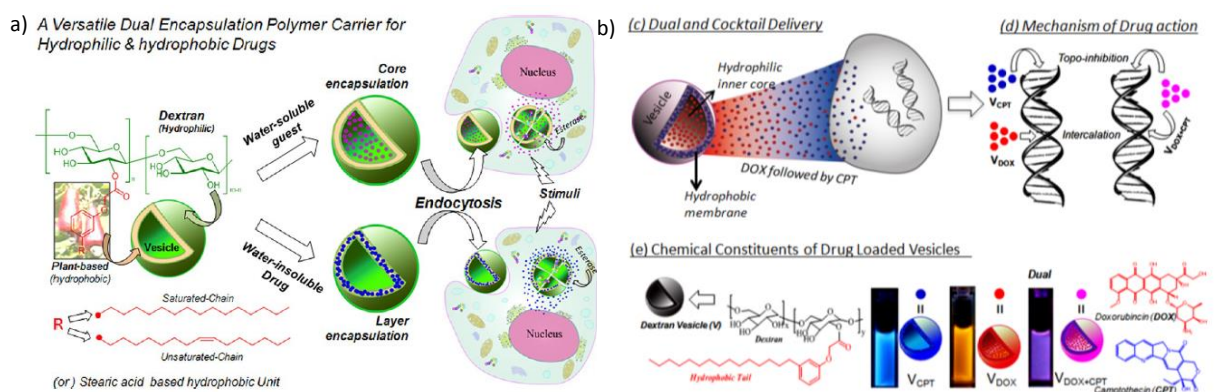


**Fig.1.4** a) Schematic of Dex-PDP vesicles encapsulation and rupture upon esterase activity. (Adopted from *Biomacromolecules* 2012, 13, 3627–3640) b) shows the dual and cocktail drug delivery. (Adopted from *Nanoscale* 2014, 6, 11841-11855)

Multi-drug delivery approach is highly important for the improvement in therapeutic efficacies of anticancer drugs in cancer therapy. Pramod *et al* was successful in achieving vesicular assembly with both water soluble DOX and water insoluble CPT drug encapsulated into a single vesicular scaffold (Fig.1.4 b)<sup>23</sup>. The intracellular esterase enzyme condition lead to the disassembly of the polymer scaffold and simultaneous release of both DOX and CPT. Further dual loaded vesicles containing both DOX and CPT showed synergistic killing in normal MEFs and cancer cells. The ratio of these drugs played crucial role in exhibiting the synergistic effect. The synergistic killing was enhanced when cocktail of CPT and DOX in the ratio of 1:4 was administered in cancer cells.

#### **1.4 pH RESPONSIVE POLYMER SCAFFOLDS**

In the above mentioned two examples the drug loaded nanoscaffolds were targeted to release drug in the tumor vicinity using the concept of EPR effect. Nevertheless the encapsulated drug should be released from the scaffold at the target site in a controlled manner. This can be achieved by exploring other significant alterations in the tumor cells including elevated temperature, lower pH and elevated redox potential etc<sup>24,25</sup>. Other than these internal alterations heat, magnetic field and light externally can be applied for the disassembly of nanoscaffolds<sup>26</sup>. These types of scaffolds which respond to particular stimuli are known as “smart or intelligent polymers”<sup>27</sup>. Therefore, the polymeric scaffold which undergoes assembly-disassembly process in response to stimuli leads to formation of efficient vectors for releasing drug in intracellular compartments. Various external stimuli such as temperature, pH, magnetic field, electric field, ultrasound etc. have been explored for administering drug at the tissue level. Among all, pH responsive scaffolds have gained tremendous attention due to lowered extracellular /interstitial pH in tumor malignancy. This characteristic of solid tumors is caused by the excessive metabolites such as CO<sub>2</sub> and lactic acid which are generally produced due to anaerobic glycolysis<sup>28</sup>. The abnormal pH gradient varies from extracellular tumor microenvironment to organelles inside the cell. One of the strategies involved in releasing drug molecules from pH responsive scaffolds includes protonation of the polymer that takes place at lower pH thereby changing the hydrophilicity of the

scaffold. As a result, disassembly of scaffold occurs and the encapsulated drug is released at the desired site. This idea has been utilized in amphiphilic polymers like PEGylated poly L-histidine<sup>29</sup>. Acid labile linkers like diorthoesters were used to conjugate hydrophobic and hydrophilic units. By adjusting either of the blocks micellar assembly was obtained and it was stable at physiological pH as well as pH above 6.5. However, at tumor pH (acidic) polymer gets protonated and rupture of self-assembly occurs thereby drug gets released. In other words, upon exposure to mild acidic condition acid labile group gets cleaved which results in disruption of the assembly.

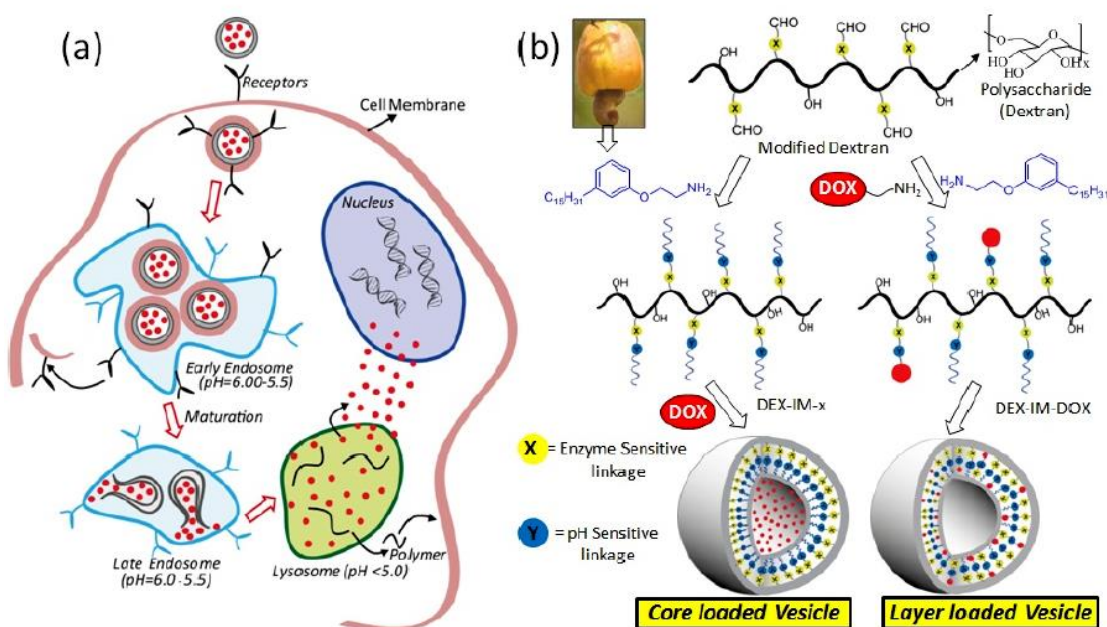


**Fig.1.5** a) Schematic of pH responsiveness inside the cell b) Synthetic design for chemically as well as physically conjugated DOX. (Adopted from Pramod et al, Nanoscale 2015, Advance article)

PEG-diorthoester-lipid conjugate, are new class of lipids which show rapid degradation at mild acidic pH conditions but are stable at physiological pH<sup>30</sup>. Other acid labile functional groups include imine, hydrazone, vinyl ether, carboxydimethylmaleic anhydride, and phosphoramidate and so on<sup>31</sup>. In this context the work done by Pramod *et al* from our research group on pH responsive vesicles is also worth mentioning. In this work, dual stimulus i.e. pH (imine linkage) and enzyme (aliphatic ester linkage) were used in designing the polysaccharide based vesicular nanoscaffolds<sup>32</sup>. Also, comparison between administrations of anticancer drug DOX to the breast cancer cells

via physical loading as well as by conjugating to the polymer backbone was investigated. Hydrophilic DOX.HCl was encapsulated in the aqueous interior to obtain core loaded vesicles and chemical conjugation of DOX resulted in DOX positioned at the hydrophobic layer of the vesicles. In vitro studies showed that under physiological conditions, these vesicles retained around 70 to 80% of the drug. On the other hand, at low pH (5-6) and in presence of esterase enzyme both the linkages were cleaved. As a result almost 100% of the loaded drug was released. The DOX physically loaded vesicles showed better cytotoxic effect than chemical conjugated one from the MTT assays.

### AIM OF THE THESIS

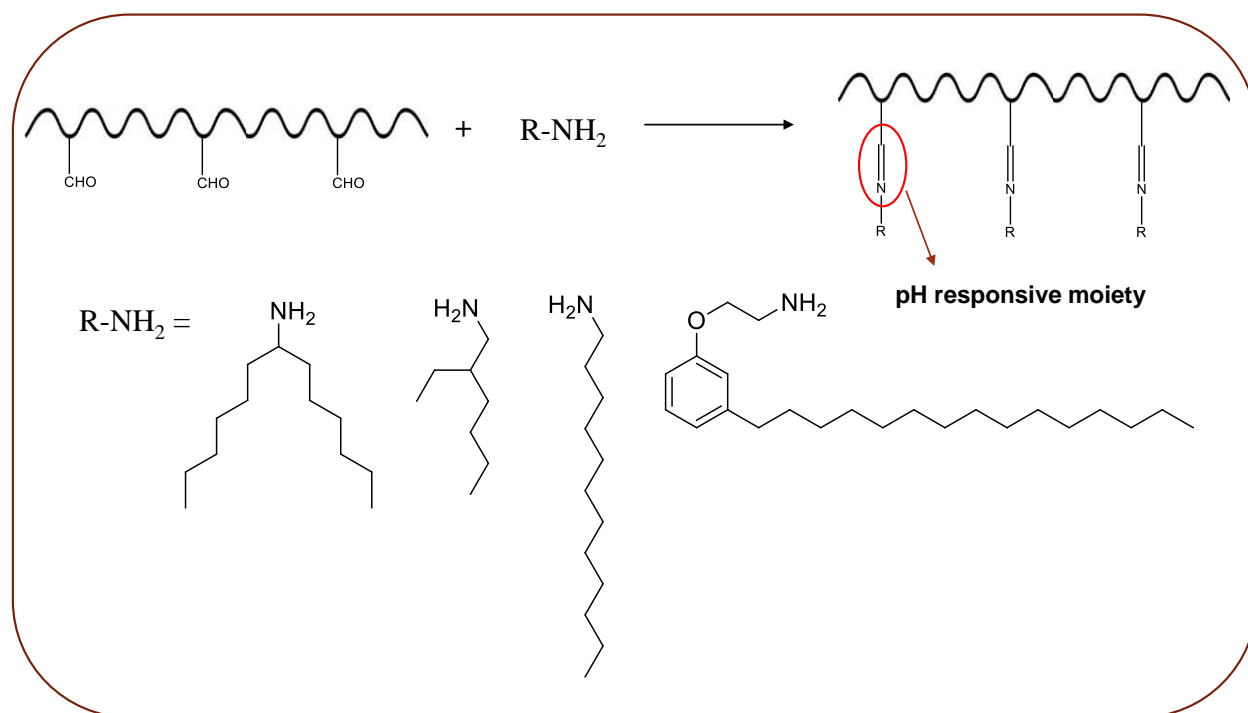


**Fig.1.5** Schematic representation of pH responsive scaffolds.

In all previous reports by Pramod *et al*, it has been shown that with 5% substitution of 3-pentadecylphenol on the dextran backbone results in the formation of vesicular assembly<sup>23</sup>. Further, these vesicular assemblies were found to exhibit dual drug loading phenomena. The dual drug loaded assemblies further showed synergistic effect thereby showing better killing effect as compared to free drug<sup>32</sup>. However, in previous all studies only pentadecylphenol derivative was used as hydrophobic segment

for grafting on dextran backbone. The role of hydrophobic units in the formation of vesicular assemblies was not investigated. Therefore present work is emphasized on studying the role of hydrophobic segment in polysaccharide based amphiphiles in formation of vesicular self-assembled structures. Further, it was also investigated that how crucial is the presence of long alkyl tail of PDP in designing of the vesicular assemblies. For this purpose, linear, branched as well as aromatic long chain hydrophobic units were chosen (Fig.1.5). Four different amines such as 1-hexylheptyl amine, 2-ethylhexyl amine, dodecyl amine and 2-(3-pentadecylphenoxy) ethanamine (PDP amine) were used for these studies.

The novelties of the present thesis can be summarized as follows; newly designed dextran amphiphiles with different hydrophobic units were synthesized through tailor made approach. The scaffolds obtained were characterized by NMR and their self-assembly was confirmed by DLS and FE-SEM techniques. The encapsulation abilities of the scaffolds were investigated using different probes such as Rh B (hydrophilic dye), Nile red and pyrene (hydrophobic dyes). The loading of these dyes were further confirmed by fluorescence technique. The in vitro release study of Rh B encapsulated Dex-PDP-IM vesicles was studied under physiological conditions.



## 2 MATERIALS AND METHODS

### 2.1 MATERIALS

Dextran ( $M_w = 6000$ ), 4-formylbenzoic acid, 3-pentadecyl phenol, di-tert-butyl-dicarbonate, ethanolamine, triphenylphosphine, diisopropyl azodicarboxylate, 2-ethyl-1-hexylamine, 4-dimethylamino pyridine, dicyclohexylcarbodiimide, rhodamine B, pyrene and nile red were purchased from sigma-aldrich . Dimethyl sulphoxide was purchased locally and distilled using  $\text{CaH}_2$  and  $\text{CaCl}_2$ . Trifluoroacetic acid and other reagents and solvents were purchased locally and purified using standard procedure prior to use.

### 2.2 METHODS

NMR was recorded in a 400MHz Jeol NMR spectrometer in  $\text{CDCl}_3$  (for ethanolamine and PDP derivatives) and  $\text{DMSO-d}_6$  (for Dextran derivatives) containing a small amount of TMS as internal standard. FT-IR spectra of all compounds were recorded on Bruker alphaT Fourier transform infrared spectrometer. Thermal stability (TGA) of synthesized compounds was checked using Perkin Elmer STA 6000 instrument. Mass of PDP derivatives and ethanolamine were confirmed using the Applied Biosystems 4800 PLUS MALDI-ToF analyzer. Absorption and release studies were performed on a Perkin Elmer Lambda 45 UV-Vis spectrophotometer. Emission studies were performed using SPEX Fluorolog HORIBA JOBIN VYON fluorescence spectrophotometer with a double grating 0.22 m spex 1680 monochromator and a 450 W Xe lamp as the excitation source at RT. The size of the Dextran derivative amphiphiles were determined by Dynamic Light Scattering (DLS) using a Nano ZS-90 apparatus using a 633nm red laser at  $90^\circ$  angle from Malvern instrument. The sample was dialyzed against water for 24 hours, the solution from the dialysis bag was diluted to obtain a concentration of 0.5mg/ml and sonicated and then filtered using 0.45 $\mu\text{m}$  filter to get a clear solution. FE-SEM images were recorded on a Ziess Ultra Plus scanning electron microscope. Samples were prepared by drop casting on a silicon wafer followed by air drying.

## 2.3 GENERAL PROCEDURES

**2.3.1 Synthesis of tert-butyl (2-hydroxyethyl) carbamate 1A:** Ethanolamine (5g, 81mmol) was dissolved in 10% sodium carbonate solution (50 ml). To this mixture, THF (5 mL) was added with continuous stirring. Di-tert-butyl- dicarbonate (21.4g, 98mmol) dissolved in THF (15ml) was added drop wise to the reaction mixture and was kept at room temperature for 12hours. The progress of the reaction was monitored by formation of white precipitate. For extraction, THF is evaporated then it is neutralized by adding 5% HCl. White precipitate disappeared. Then the reaction mixture is extracted with ethyl acetate and little amount of sodium sulphate is added. Filter it and separate the organic layer from aqueous layer and evaporate the organic solvent. It was purified by passing through silica gel column of 60-120 mesh using 25% ethyl acetate-pet ether as eluent. Yield=8.82g (75%). MALDI-ToF-MS, (MW=161),m/z = 200 (M<sup>+</sup>+K<sup>+</sup>) and 184 (M<sup>+</sup>+Na<sup>+</sup>).<sup>1</sup>H NMR (400MHz, CDCl<sub>3</sub>) δ: 4.99 ppm (s, 1H, -NH), 3.68 ppm (t, 2H, -CH<sub>2</sub>-CH<sub>2</sub>-OH), 3.25 ppm (t, 2H,-CH<sub>2</sub>-CH<sub>2</sub>-OH), 1.42 ppm (s, 9H, tert-butyl group).

**2.3.2 Synthesis of tert-butyl (2-(3-pentadecylphenoxy)ethyl)carbamate 1B:** Pentadecylphenol (5.62g, 18.6mmol) was taken in a 250ml 2 neck round bottom flask. Add 1A (3g, 18.6mmol) and triphenylphosphine (5.34g, 20.4mmol) to it. Purge with nitrogen for 10-15 minutes. Dry THF (40 ml) was added to the reaction mixture. It was then stirred for 10-15 minutes in ice cooled bath and again purges it with nitrogen for 15 minutes. Then add Di isopropyl azodicarboxylate (DIAD, 3.62ml) drop by drop to the reaction mixture. After 5 minutes ice bath was removed and kept it for stirring at room temperature for 24 hours. It was purified by passing through silica gel column of 60-120 mesh using 1% ethyl acetate-pet ether as eluent. Yield = 6.5g (78%). <sup>1</sup>H NMR (400Mz CDCl<sub>3</sub>) δ: 7.18 ppm (t, 1H, Ar-H), 6.8ppm (d, 1H, Ar-H), 6.72ppm (s,1H,Ar-H), 6.70ppm (d, 1H, Ar-H),5 ppm (s, 1H, N-H), 4.02ppm(t, 2H, NH-CH<sub>2</sub>-CH<sub>2</sub>-O), 3.53ppm (t, 2H, NH-CH<sub>2</sub>-CH<sub>2</sub>-O),2.57ppm (t, 2H, Ar- CH<sub>2</sub>), 1.60ppm (m, 2H, Ar- CH<sub>2</sub>-CH<sub>2</sub>),1.46ppm (s, 9H, t-butyl group), 1.28ppm (m, 27H, Aliphatic protons),0.87ppm (t, 3H, Ar-(CH<sub>2</sub>)<sub>14</sub>-CH<sub>3</sub>).MALDI-ToF-MS, (MW= 447.62),m/z = 486 (M<sup>+</sup>+K<sup>+</sup>) and 470 (M<sup>+</sup>+Na<sup>+</sup>).

**2.3.3 Synthesis of 2-(3-pentadecylphenoxy)ethanamine 1C:** 1B (1g, 2.22mmol) was dissolved in 10ml of Dichloromethane and adds about 5.2 ml of Trifluoroacetic Acid (TFA) to it. Immediately after the addition of TFA color of the reaction mixture changes from pale brown to dark brown color. Then the reaction mixture is stirred for an hour. After one hour Dichloromethane is evaporated from the reaction mixture. Along with Dichloromethane, TFA will also get evaporated. To remove TFA completely add some more Dichloromethane to the mixture and evaporate it again. Repeat this for 2-3 times. The amine salt is extracted using adding diethyl ether (20ml) to the reaction mixture which is placed in ice bath. It was purified by passing through silica gel column of 60-120 mesh using chloroform-methanol solvent system as eluent. Yield=0.6935g (89%).<sup>1</sup>H NMR (400Mz CDCl<sub>3</sub>) δ: 7.15 ppm(t, 1H, Ar-H), 6.76ppm (d, 1H, Ar-H), 6.72ppm (s,1H, Ar-H),6.69ppm (d, 1H, Ar-H), 3.97 ppm (t,2H,O-CH<sub>2</sub>), 3.08ppm (t, 2H,O-CH<sub>2</sub>-CH<sub>2</sub>), 2.55ppm (t, 2H, Ar-CH<sub>2</sub>), 1.58ppm (m, 2H, Ar-CH<sub>2</sub>-CH<sub>2</sub>), 1.28ppm (m, 27H, aliphatic protons), 0.87ppm (t, 3H, -CH<sub>3</sub>).MALDI-ToF-MS: (MW=345.52):m/z = 384.28(M<sup>+</sup>+K<sup>+</sup>) and 368.31(M<sup>+</sup>+Na<sup>+</sup>).

**2.3.4 Synthesis of Dex-CHO-x:** Dextran (1g, 6.21mmol of anhydroglucose unit) and 4-formyl benzoic acid (0.466g, 3.105mmol, for Dex-CHO-12) were dissolved in anhydrous DMSO (20 mL) and the solution was then purged for 15 minutes with dry nitrogen. Dicyclohexylcarbodiimide (0.96g, 4.65mmol) and 4-(dimethylamino) pyridine (0.076g, 0.621mmol) were dissolved independently in anhydrous DMSO (3ml) and were added into the reaction mixture. The reaction was stirred for an hour under N<sub>2</sub> purging and then reaction was continued at 25<sup>o</sup>C under nitrogen atmosphere for 24 hours. Dicyclohexyl urea was removed by filtrating and the solvent was removed using vacuum distillation (0.1mm Hg). The thick viscous liquid was then precipitated in methanol (100 mL). The solid was filtered and washed several times using acetone and methanol. The product was then filtered out and dried under vacuum at 60<sup>o</sup>C. Yield = 60%. <sup>1</sup>H NMR (400 MHz, DMSO-d<sub>6</sub>): δ = 10.08ppm (s, 1H, -CHO), 8.16ppm (d, 2H, Ar-H adjacent to aldehyde group), 8.02ppm (d, 2H, Ar-H), 4.47, 4.82, 4.88 (s, hydroxyl of dextran), 4.63ppm (s, dextran anomeric proton), 3.14-3.69ppm (dextran glucosidic protons).

**Dex-CHO-x** with different degrees of substitutions i.e. Dex-CHO-1, 3, 6, 9, 12 and 20 were synthesized by changing the mole ratios of 4-formylbenzoic acid to dextran as 0.25, 0.5, 0.75, 1, 1.5 and 2 in the feed.

**2.3.5 Synthesis of Dex-PDP-IM:** PDP-amine (1C) (0.25g, 0.674mmol) was dissolved in anhydrous DMSO (10ml). To this sodium carbonate (0.1g) was added and purged with dry N<sub>2</sub> for 15 min. To the above solution, Dex-CHO-12 (1g) in anhydrous DMSO (20ml) was added. The reaction was then purged for 15 min and heated at 50°C under N<sub>2</sub> atmosphere for 4 hours. Solution was filtered and DMSO was removed under vacuum to obtain a thick viscous liquid. This was then precipitated in cold methanol to get the product. Purification was done using reprecipitation technique and washing with cold methanol several times. The final product was then collected after filtration and dried under vacuum at 50°C. Yield = 60%. <sup>1</sup>H NMR (400 MHz, DMSO-d<sub>6</sub>) δ: 8.48 ppm (s, 1H, imine proton), 7.63 ppm (d, 2H, Ar-H adjacent to imine linkage), 6.93 ppm (d, 2H, Ar-H), 8.01 ppm (d, 2H, Ar-H of 4-formylbenzoic acid unit), 7.84 ppm (d, 2H, Ar-H of 4-formylbenzoic acid unit), 7.10 ppm (s, 1H, Ar-H of PDP unit), 6.70 ppm (m, 3H, Ar-H of PDP unit), 4.47, 4.82, 4.88 ppm (s, hydroxyl groups of dextran), 4.63 ppm (s, anomeric proton of dextran), 3.14-3.69 ppm (glucosidic protons of dextran), 4.14 ppm (t, 2H, O-CH<sub>2</sub> of PDP unit), 3.81 ppm (t, 2H, O-CH<sub>2</sub>-CH<sub>2</sub> of PDP unit), 1.46 ppm (m, 2H, Ar-CH<sub>2</sub>-CH<sub>2</sub>), 1.17 ppm (m, 27H, aliphatic protons), 0.79 ppm (t, 3H, -CH<sub>3</sub>).

Similar procedure was adopted for the synthesis of other derivatives like Dex-Dod-IM, Dex-EH-IM and Dex-HH-IM by using different amines such as Dodecyl amine, 2-ethylhexyl amine and 1-hexylheptyl amine respectively.

**2.3.6 Determination of Critical Vesicular Concentration (CVC):** Pyrene was used as a fluorescent probe to determine the critical vesicular concentration of the synthesized polymer. In this experiment, 1 ml of pyrene (0.6 μM) in acetone was added to 5 ml glass vials and the acetone was allowed to air dry completely. Concentrations of Dex-PDP-IM was varied from 0.5 mg/ml to 0.00083 mg/ml and was added to these vials. Then the vials were sonicated for one hour and the samples were kept overnight for equilibration. The excitation wavelength was set to be at 337 nm. The excitation and emission slit width were fixed as 1.5 nm and 3 nm respectively. The ratio of fluorescence intensity at

I<sub>1</sub> (372 nm) and I<sub>3</sub> (383 nm) was plotted against the logarithm of concentration to get a graph where the onset of the slope gives the CVC.

**2.3.7 Encapsulation of a hydrophilic Rhodamine B (Rh B) and determination of loading efficiency in Dex-IM derivatives:** The ability of synthesized Dex-imines to stabilize hydrophilic dye Rh B was studied using the solvent exchange/dialysis method. 20 mg of the polymer and 2 mg of Rh B were taken in a 5 ml beaker and was dissolved in 2 ml of DMSO. Then 2 ml of distilled water was added drop wise into the stirring solution and further it was stirred at 25<sup>o</sup>C for 12 hours. The solution was transferred into a dialysis bag (MWCO = 3500) and dialyzed against water until the leaching of Rh B from the dialysis bag has stopped completely. 100 µl of the dialyzed solution was diluted into 3 ml using DMSO. The dye loading content and efficiency was determined from beers law where molar absorptivity coefficient of dye was fixed as 116,000.

$$\text{DLE (\%)} = (\text{weight of dye in vesicles/weight of dye in the feed}) \times 100\%$$

$$\text{DLC (\%)} = (\text{weight of dye in vesicles/weight of dye loaded vesicles}) \times 100\%$$

**2.3.8 Encapsulation of hydrophobic dye pyrene in Dex-IM derivatives:** 20 mg of the polymer and 2 mg of Pyrene were taken in a 5 ml beaker and was dissolved in 2 ml of DMSO. Then 2 ml of distilled water was added drop wise into the stirring solution and further it was stirred at 25<sup>o</sup>C for 12 hours. The solution was transferred into a dialysis bag (MWCO = 3500) and dialyzed against water for 24 hours at 25<sup>o</sup>C. The dye loading content and efficiency was determined from beers law where molar absorptivity coefficient of dye was fixed as 54,000.

Similarly, Nile red was also encapsulated in Dex-IM derivatives. The procedure followed for the encapsulation studies was similar to pyrene encapsulation except that Nile red precipitates out in the dialysis bag if it's not getting stabilized by the scaffold. Therefore, dialyzed solution was filtered before taking the absorbance.

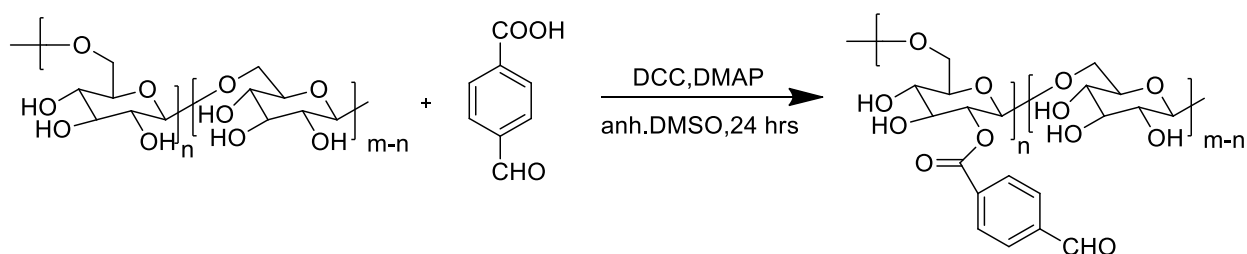
**2.3.9 *In-vitro* Release studies:** The dye release study from the Dex-PDP-IM vesicle was investigated at pH 7.4 (physiological pH), pH 5.5 (endosomal pH) and pH 2 (extreme acidic pH). In a typical experiment, 3 mg of Dex-PDP-IM vesicle encapsulated with Rh B in 3 ml PBS buffer solution of desired pH were placed in dialysis tube (MWCO

= 3500). The tube carrying Rh B loaded Dex-PDP-IM vesicle was immersed in 100 ml buffer solutions having corresponding pH of reconstituted buffer taken in a beaker. The release studies were performed at 37°C (physiological temperature) by incubating solutions. At regular time intervals (30 min or 60 min) 3 ml of dialysis medium was taken and replaced with equal amount of fresh buffer. Using UV-Vis absorption spectrophotometry, absorbance of each aliquot was recorded and amount of the dye released were calculated by Beer's law.

### 3 RESULTS AND DISCUSSION

#### 3.1 SYNTHESIS OF Dex-CHO-x AND CHARACTERIZATION

Dextran ( $M_w = 6000$ ), a biocompatible and biodegradable polymer consists of linear  $\alpha$  (1-6) linked glucose units and  $\alpha$  (1-3) link initiated branches. Dextran was coupled with 4-formylbenzoic acid by DCC/DMAP coupling to achieve aldehyde functionality grafted to the dextran backbone, which can be further utilized for iminization reaction (Scheme 3.1).  $^1\text{H}$  NMR spectrum of Dex-CHO showed peaks at 10.08 ppm corresponding to aldehyde proton (Ar-CHO). While peaks at 8.02 and 8.16 ppm belongs to aryl protons. The peak at 4.63 ppm corresponds to anomeric proton and 4.47, 4.82, 4.88 ppm belongs to hydroxyl groups of dextran. Whereas 3.14-3.69 ppm belongs to dextran glucosidic protons. Upon formation of ester linkage, the proton Ar-COO-CH appeared at 5.26 ppm which confirms that coupling has occurred. Moreover, slight shift in aryl protons as well as aldehyde proton has observed after coupling with respect to the monomer spectrum of 4-formylbenzoic acid. i.e. 8.01, 8.12 ppm to 8.02, 8.16 ppm in the case of aryl protons and 10.06 ppm to 10.08 ppm in the case of aldehyde proton gives additional evidence that esterification has happened (Fig 3.1). The degree of substitution (DS) was calculated in Dex-CHO-x by comparing the peak intensities of anomeric proton of dextran at 4.63 ppm with aldehyde proton at 10.08 ppm.



Scheme 3.1 Synthesis of Dex-CHO-x

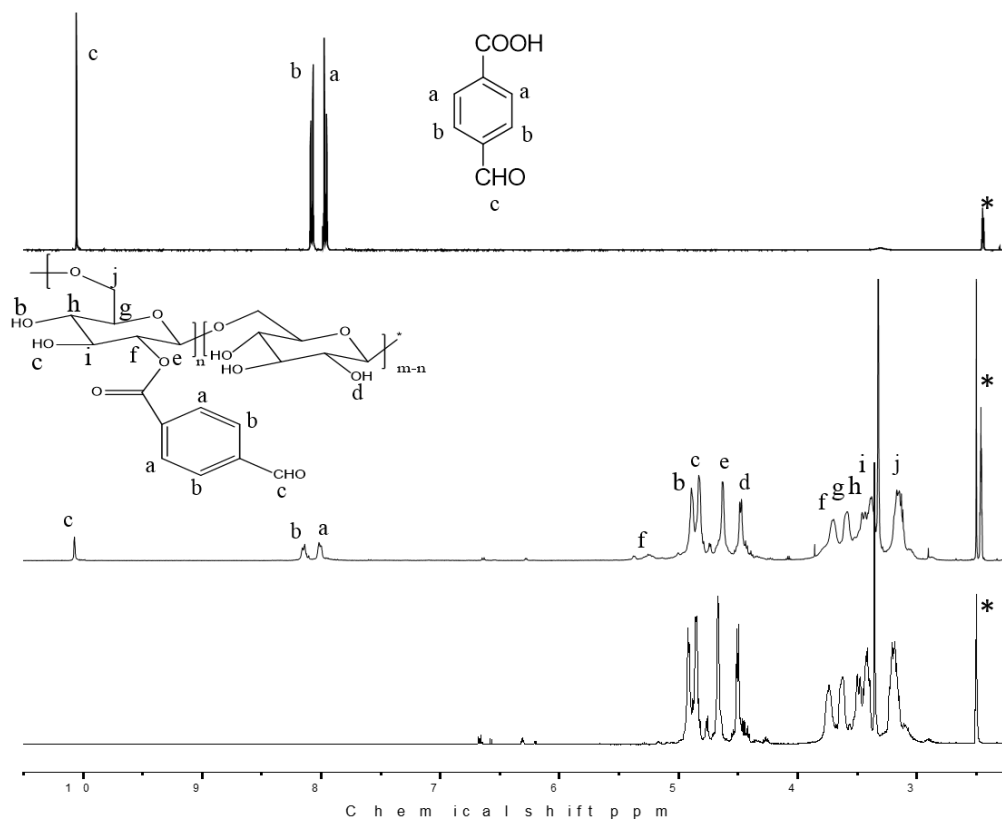


**Fig. 3.1**  $^1\text{H}$  NMR spectra of Dex, Dex-CHO and 4-formylbenzoic acid in DMSO-d<sub>6</sub>.

DS = (Integral value at 10.08 ppm/Integral value at 4.63 ppm)  $\times$  100. DS in Dex-CHO-x were obtained as 1, 3, 6, 9, 12 and 20% for the feed ratio of 0.25, 0.5, 0.75, 1, 1.5 and 2 equivalents of 4-formylbenzoic acid (Fig. 3.2 & Table 3.1).

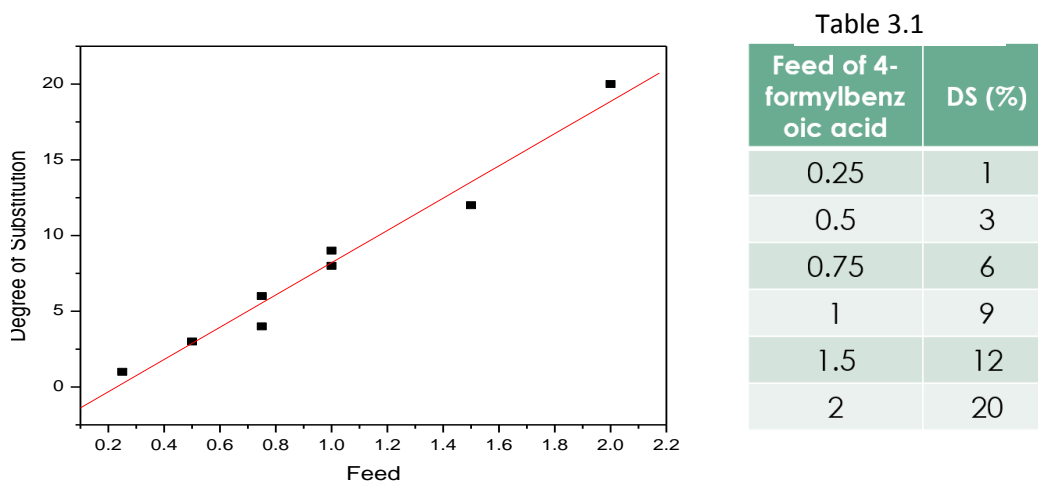


**Fig. 3.2** Plot of actual incorporation versus the mole percent of 4-formylbenzoic acid in the feed.



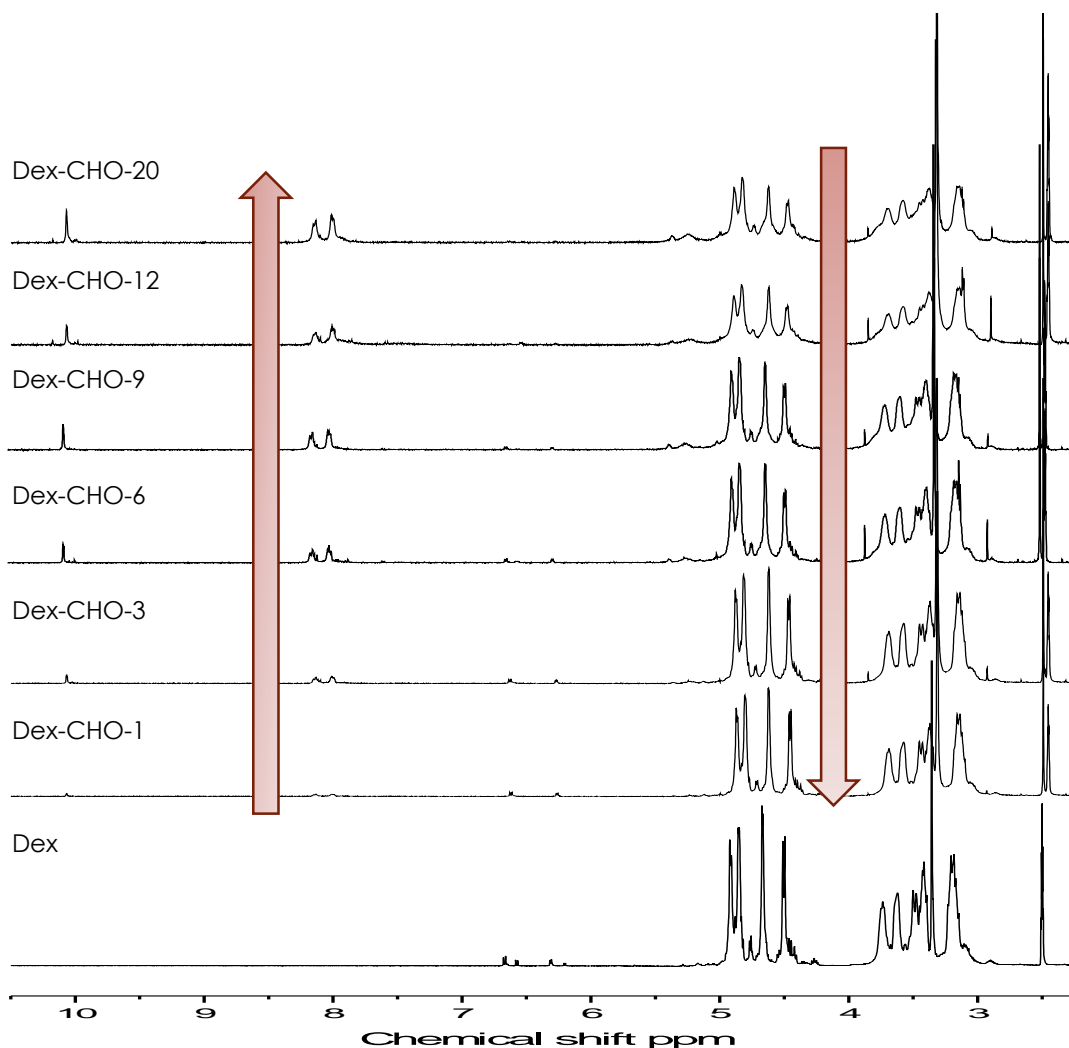


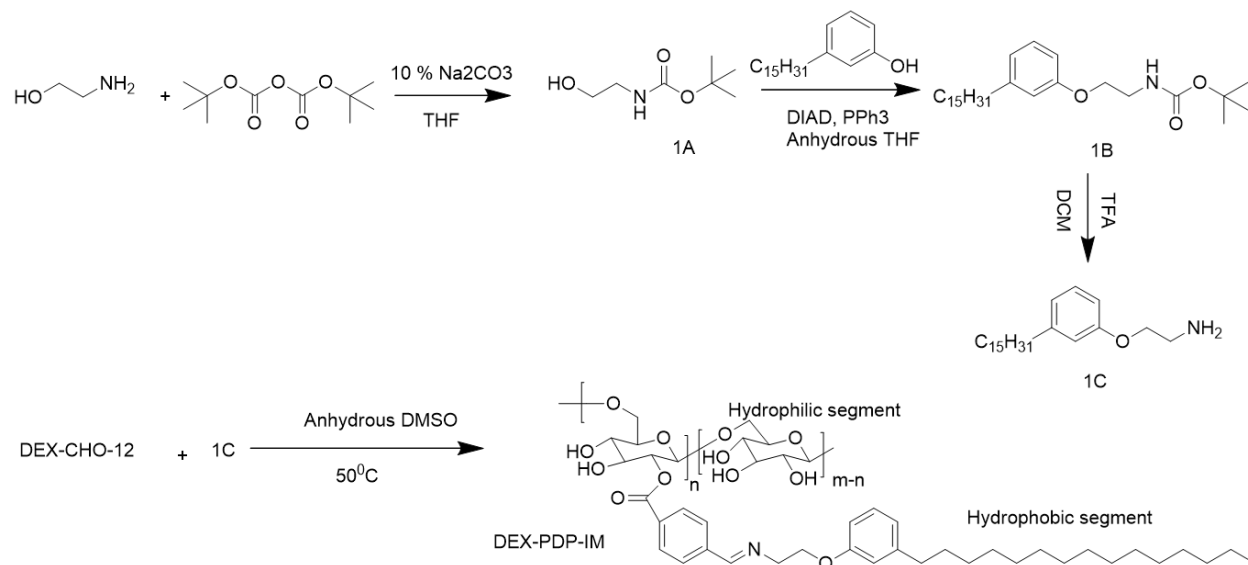
**Fig. 3.3** <sup>1</sup>H NMR of Dextran and Dex-CHO-x in DMSO-d<sub>6</sub>.

A plot of feed of 4-formylbenzoic acid versus degree of substitution showed a linear trend. As the feed of 4-formylbenzoic acid increases, the degree of substitution increases as well. And the reproducibility of these reactions were checked and found that degrees of substitution obtained were more or less the same (Fig 3.2).

Fig. 3.3 shows that intensity of aromatic peaks as well as aldehyde peaks increases upon increasing the substitution. And also the peak at 4.47 ppm which corresponds to one of the hydroxyl proton decreases upon increasing substitution implies that the aldehyde unit is getting grafted at this position. From various degree of substitutions of Dex-CHO-x, Dex-CHO-12 has been chosen for further iminization reactions because

higher degree of substitution can lead to solubility issue and lower substitutions makes hard to quantify from NMR characterizations.

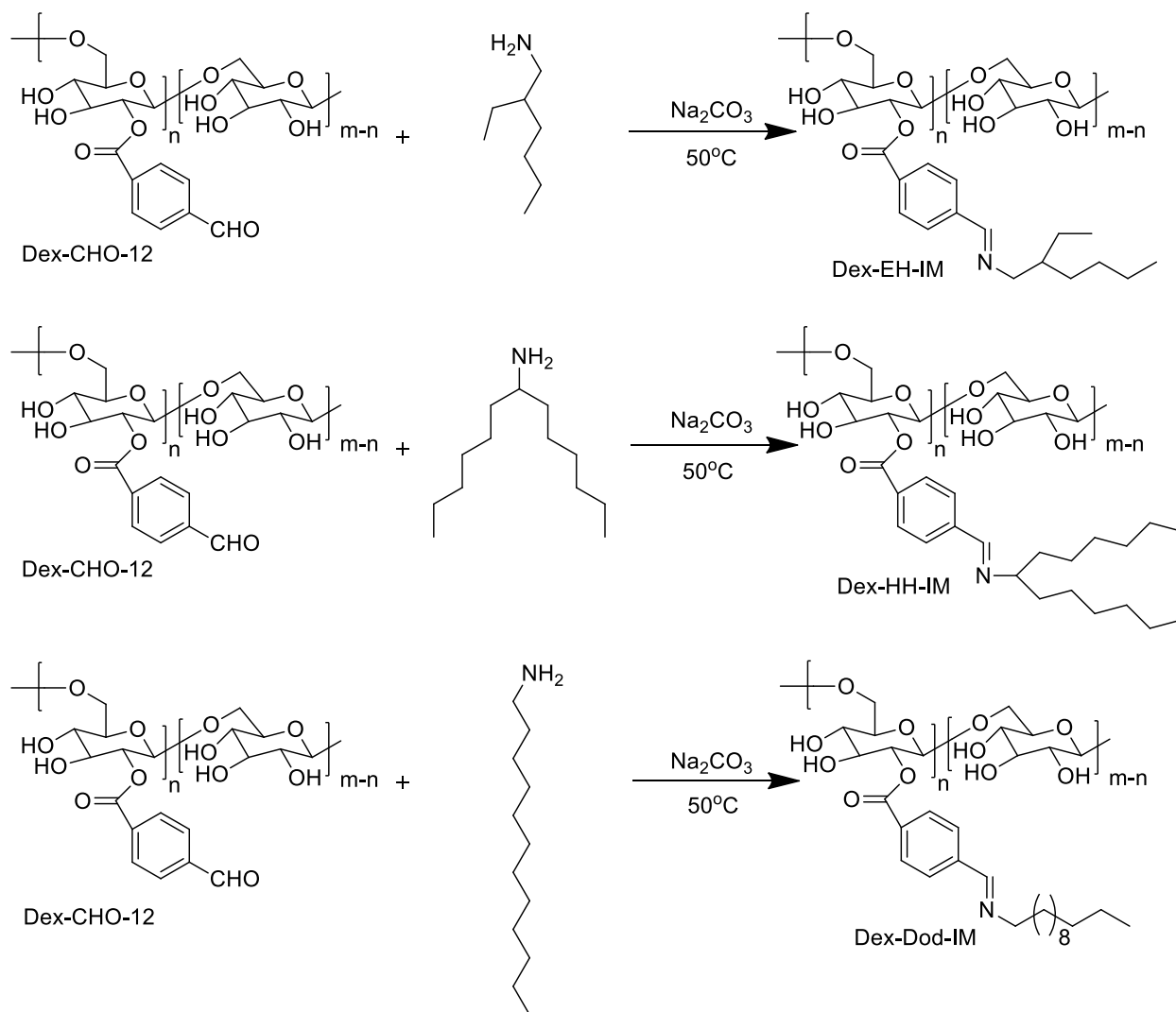
### SYNTHESIS OF pH RESPONSIVE AMPHIPHILES (Dex-IM)



Scheme 3.2 Synthesis of Dex-PDP-IM

The dextran bearing aldehyde with 12% degree of substitution (Dex-CHO-12) was further coupled with different hydrophobic units containing amines using simple iminization reaction. The reaction was carried out at 50°C in presence of sodium carbonate. Different amines used for iminization reactions were 2-ethylhexyl amine, 1-hexylheptyl amine, dodecyl amine and PDP amine. Synthetic scheme for the synthesis of Dex-PDP-IM is shown in scheme 3.2. The <sup>1</sup>H NMR of Dex-PDP-IM shows a new peak around 8.41 ppm corresponding to a characteristic imine peak and also aldehyde proton peak around 10.08 ppm was vanished after the iminization reaction indicating the formation of the desired product. Synthetic schemes for other imine derivatives are shown in scheme 3.3. In case of Dex-Dod-IM, new imine peak appeared at 8.39 ppm. Apart from characteristic imine peak, peaks corresponding to the terminal -CH<sub>3</sub>, 20 aliphatic and -CH=N-CH<sub>2</sub>-CH<sub>2</sub>- proton appeared at 0.80, 1.25 and 1.57 ppm respectively. Whereas for Dex-EH-IM, peaks appeared at 0.84, 1.30, 1.57 and 2.63 corresponds to -CH<sub>3</sub> (6H), -CH<sub>2</sub> (8 protons), N-CH<sub>2</sub>-CH- and N-CH<sub>2</sub>-CH- respectively. Apart from that new peak emerged at 8.39 ppm and aldehyde peak got vanished.

Similar trend was observed in case of Dex-HH-IM derivatives i.e. the vanishing of aldehyde peak and appearance of new characteristic imine peak around 8.4 ppm (Fig 3.4).



Scheme 3.3 Synthetic scheme of Dex-IM derivatives.

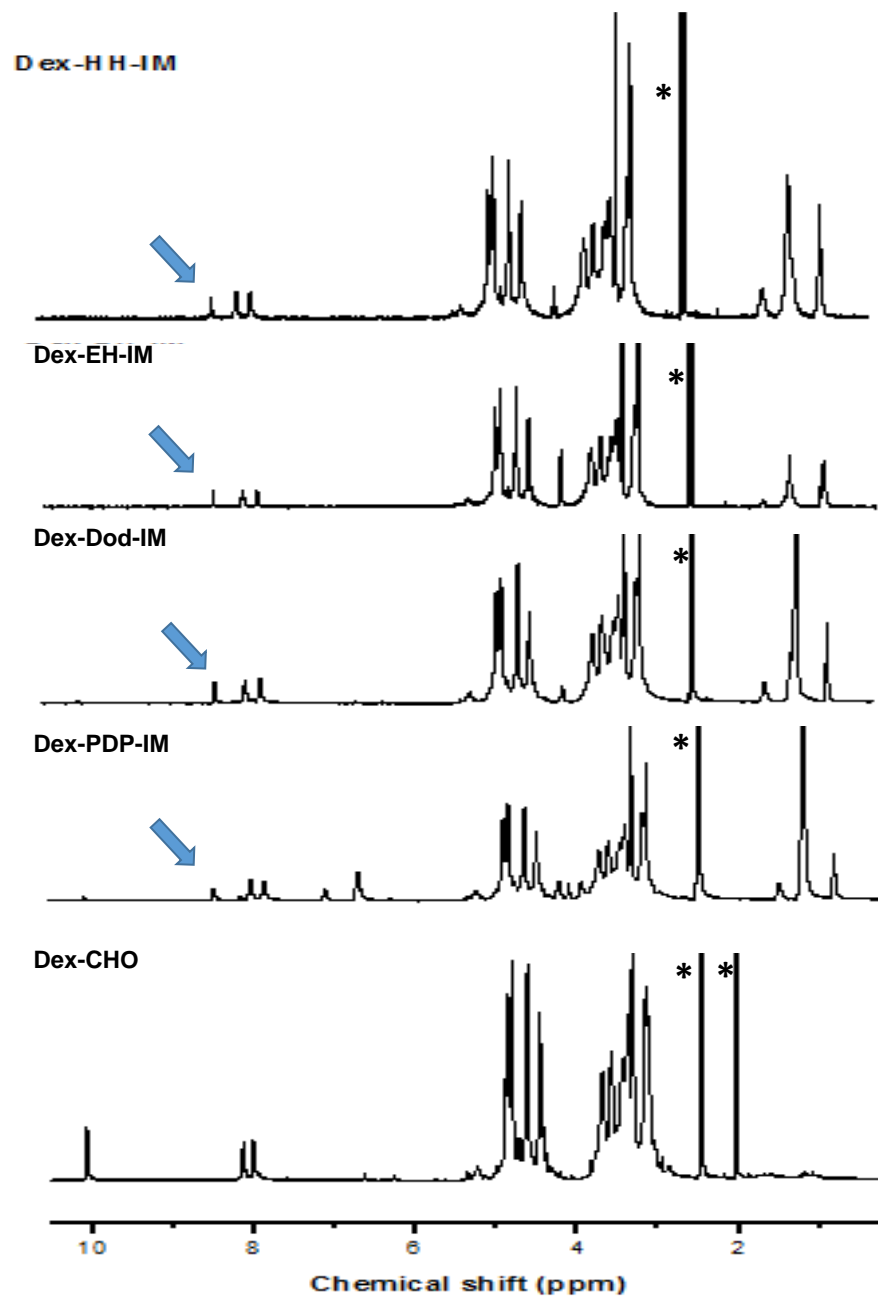


**Fig.3.4** <sup>1</sup>H NMR of Dex-IM derivatives in DMSO-d<sub>6</sub>.

### 3.2 SELF ASSEMBLY OF Dex-IM DERIVATIVES

The self-assembly of the Dex-PDP-IM derivatives in aqueous medium was further studied using dynamic light scattering technique. The DLS histograms of the aggregates formed by Dex-PDP-IM derivatives are shown in the Fig.3.5. The DLS profile of all the imine derivative of dextran showed monomodal distribution with average sizes ranging from 120-200 nm depending on the hydrophobic unit present in it.

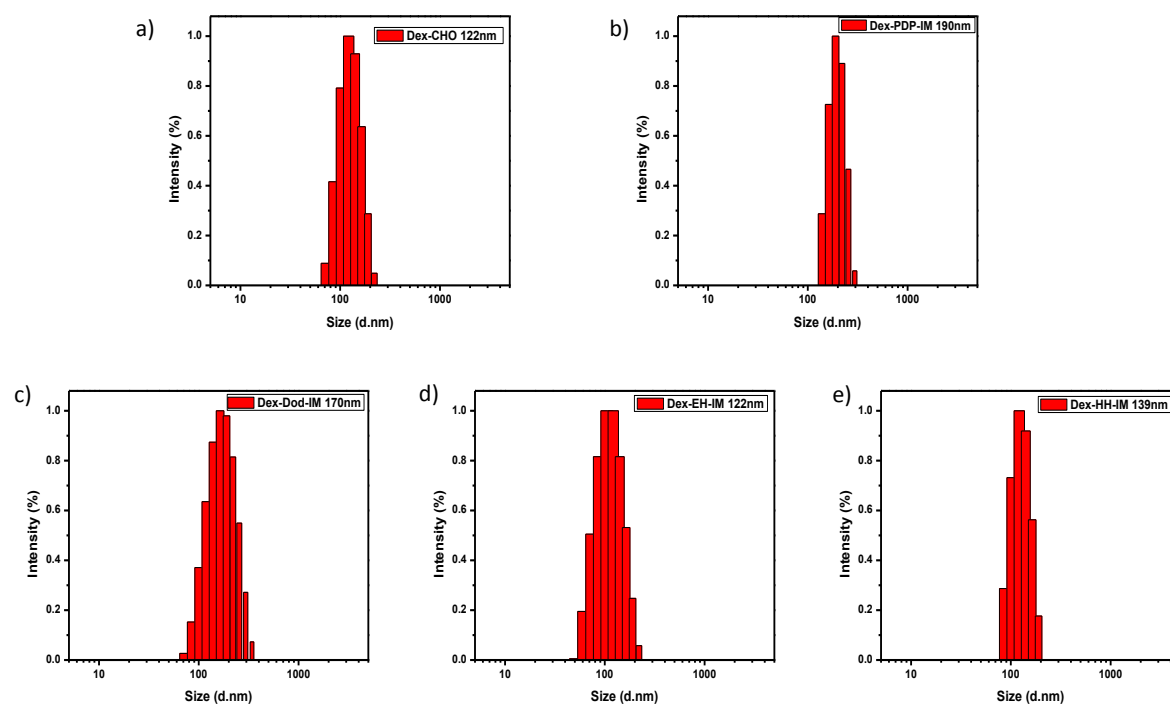


**Fig.3.5** DLS histograms of Dex-IM derivatives at 0.5 mg/ml concentration in water.

In order to visualize the morphology of the aggregates formed by imine functionalized dextran derivatives, the aqueous solution of all the derivatives was subjected to field emission scanning electron microscopy (FE-SEM) analysis. FE-SEM images of Dex-PDP-IM and Dex-Dod-IM are shown in Fig.3.6. The FE-SEM images of Dex-PDP-IM (Fig 3.6a and 3.6b), showed the formation of spherical aggregates with outer bright hydrophobic layer inner hydrophilic layer. Thus from FE-SEM images it is evident that aggregates formed by Dex-PDP-IM are vesicular assemblies. Whereas, in case of Dex-Dod-IM formation of spherical nanoparticles was observed.

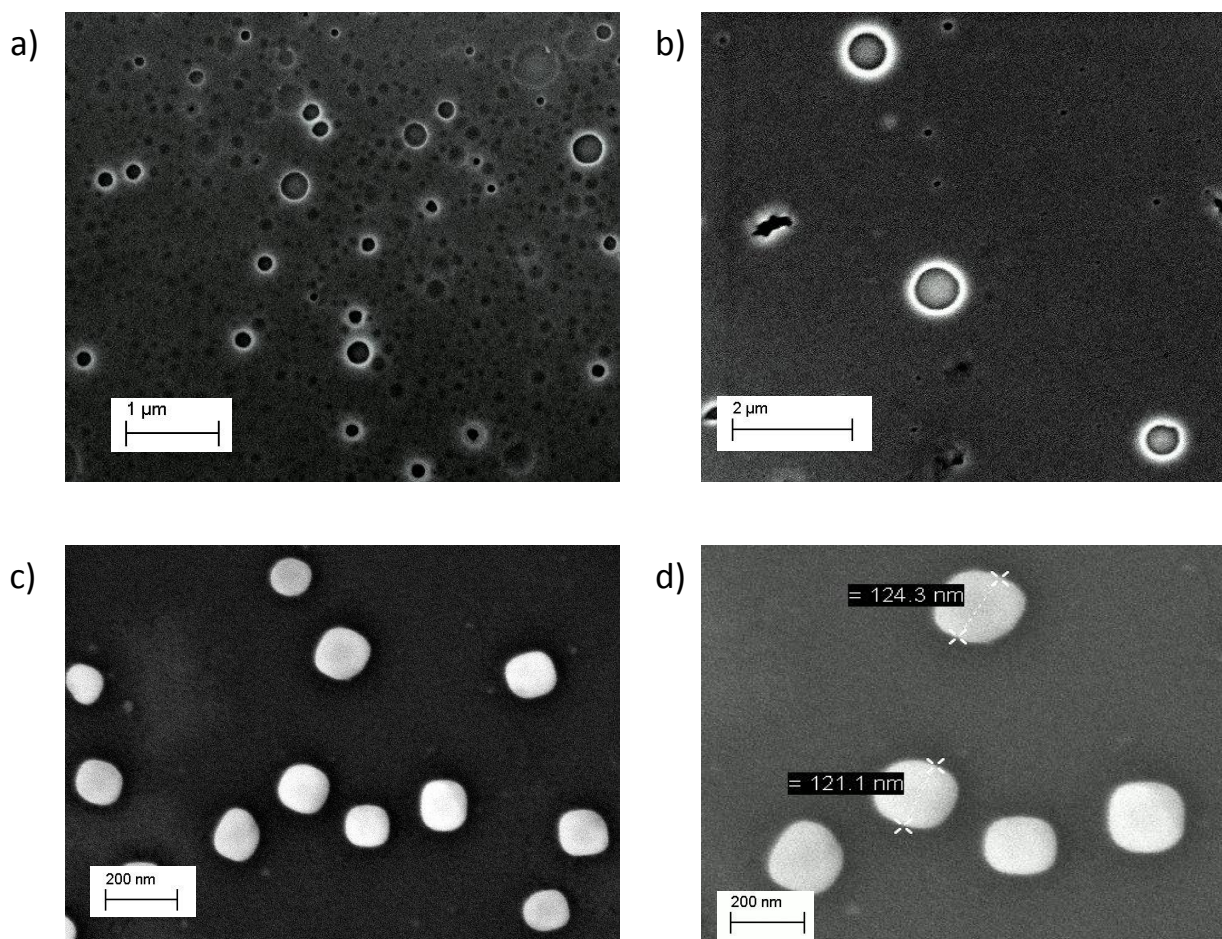


**Fig.3.6** FE-SEM images of Dex-PDP-IM (a & b) and Dex-Dod-IM (c & d).

### **DETERMINATION OF CRITICAL VESICULAR CONCENTRATION (CVC)**

CVC of the polymer is the concentration above which the individual amphiphiles self-assemble to form vesicles. Since pyrene is sensitive to its micro-environment, the critical vesicular concentration of Dex-PDP-IM was determined using pyrene as a fluorescent probe. Being a hydrophobic dye, pyrene gets localized in the hydrophobic layer of vesicle. The ratio of intensities of first ( $I_1$ , 372nm) and third vibrational bands ( $I_3$ , 383nm) are generally used to show the correlation with solvent polarity. For CVC determination, the pyrene concentration was fixed (0.6  $\mu\text{M}$ ) whereas polymer concentration was varied gradually. The emission spectra of pyrene loaded Dex-PDP-IM is shown in Fig. 3.7. The ratio of  $I_1/I_3$  as a function of concentration was plotted (see Fig 3.7b). It was observed that with the increase in polymer concentration

the ratio of  $I_1/I_3$  decreases from 2.0 to 1.2. Since the  $I_1/I_3$  value were obtained in the range of  $1 < I_1/I_3 < 1.5$ , it indicated that pyrene was encapsulated in the hydrophobic layer of the vesicles. Thus, Dex-PDP-IM self-assembles to form vesicles thus pyrene prefers to stay in the hydrophobic region of vesicle. Further, plot of logarithmic of concentration versus  $I_1/I_3$  ratio shows a sigmoidal curve. The onset of the slope was chosen as the CVC since that indicates the beginning of association event. The CVC for Dex-PDP-IM was found to be  $1.67 \times 10^{-5}$  M.

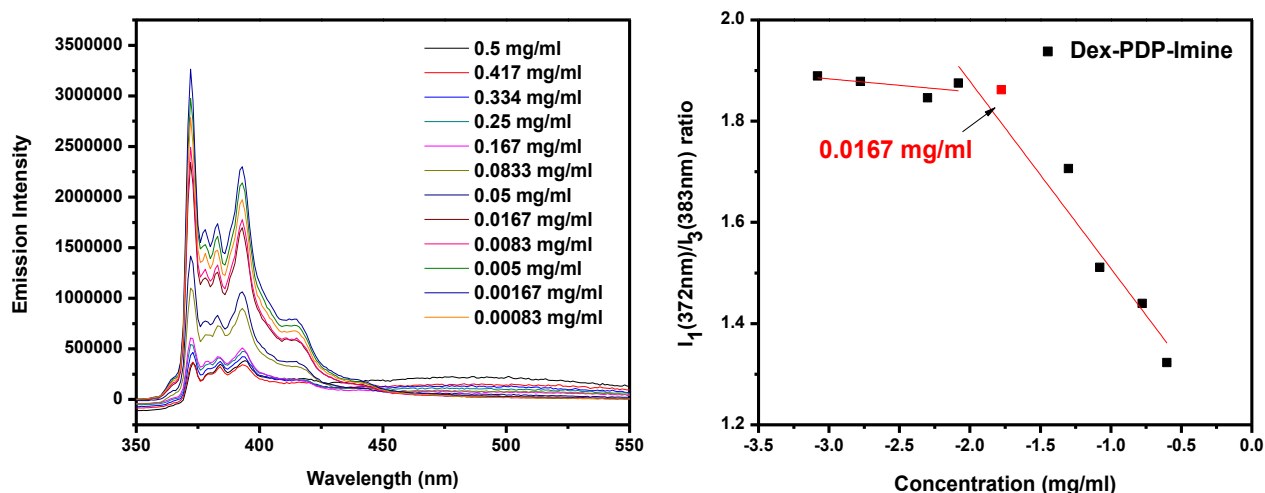


**Fig. 3.7** a) Emission spectrum of pyrene Dex-PDP-IM. b) CVC value for Dex-PDP-IM

### 3.3 ENCAPSULATION STUDIES

#### 3.3.1 Rhodamine B as hydrophilic dye

Rh B, a highly fluorescent hydrophilic dye was chosen to investigate more about the interior of vesicle. Due to its hydrophilicity, it was presumed that Rh B gets localized in the internal layer of vesicles. The scaffold's capability of stabilizing the hydrophilic dye was tested by dialyzing the solution containing dye and polymer against water. The water was replaced at regular intervals and the unencapsulated dye was removed by this method. The solution was further dialyzed until the leaching stops completely. This experiment was done for four different Dex-IM derivatives and Dex-CHO. None of the polymer except Dex-PDP-IM stabilized the hydrophilic dye Rh B. This implies that only the Dex-PDP-IM scaffold could self-assemble in water to form vesicles. In the case of

other scaffolds Rh B leached out completely within 24 hours. It can be reasoned out with two reasons, Pentadecylphenol having long aliphatic chains packs properly because of the interdigitation of the alkyl chains in the scaffold and thus self-assemble into vesicles (from the crystal structure and thermal analysis of the hydrophobic units)<sup>32</sup>.

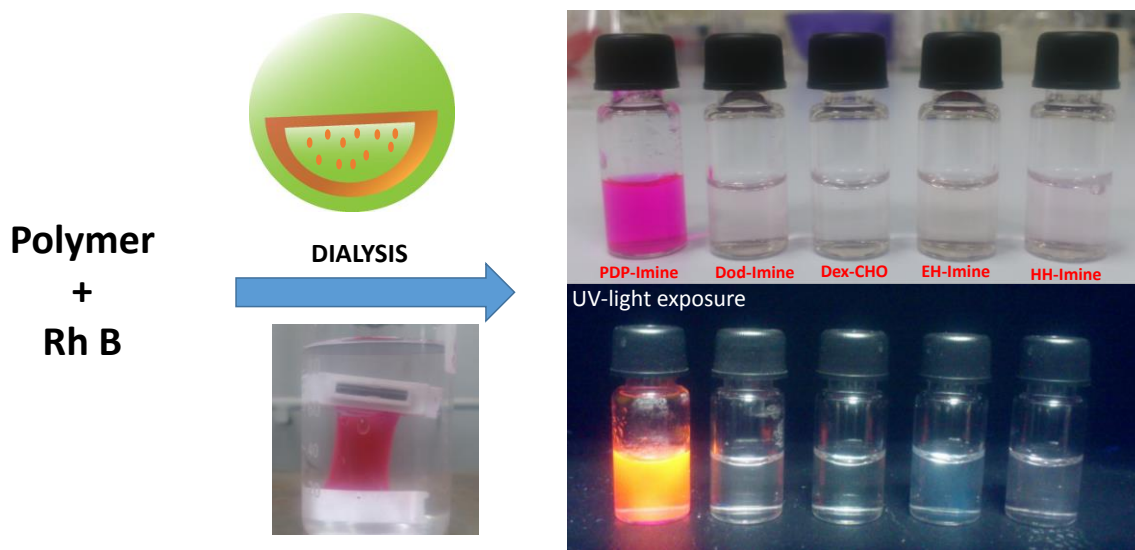


**Fig. 3.8** Rh B encapsulated scaffolds under white light and upon photo excitation.

The dye loading content for Dex-PDP-IM was calculated using Beers law and was found to be 0.46 wt%. This experiment confirms the formation of vesicular assembly for Dex-PDP-IM since micelles or nanoparticles cannot afford Rh B in its hydrophobic core. Rh B loaded Dex-PDP-IM was further characterized using Dynamic Light Scattering. DLS size showed that there is no appreciable change in size of the nascent scaffold after the encapsulation. The DLS size was found to be  $D_n = 190\text{nm}$  (Fig. 3.9 a). The Rh B encapsulation was further supported by fluorescence microscopy where the fluorescence was observed from the encapsulated Rh B (Fig. 3.9 b).



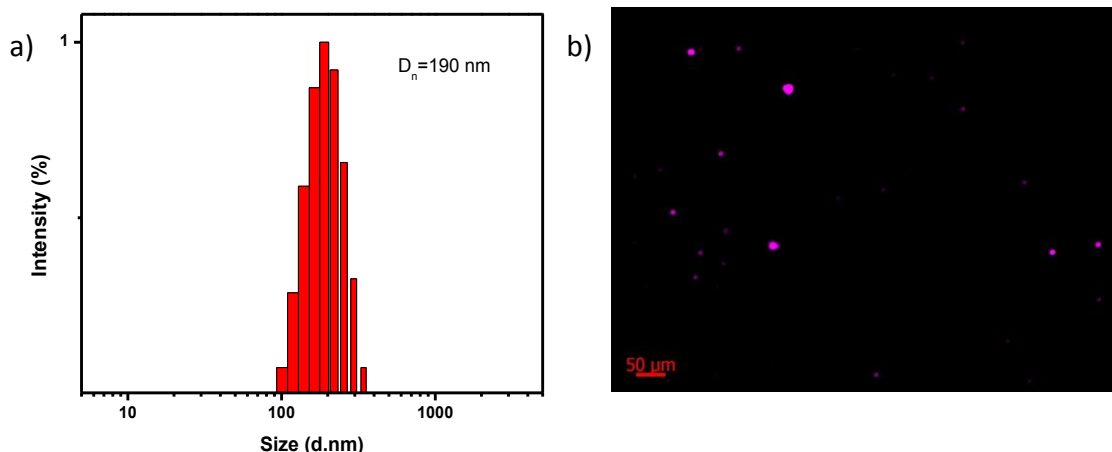


**Fig.3.9** a) DLS profile and b) Fluorescence microscopy of Rh B encapsulated Dex-PDP-IM.

### 3.3.2 Nile Red as hydrophobic dye

Nile Red another fluorescent probe was used to get the insight about the hydrophobic core of vesicles. It was hypothesized that Nile Red dye can get localized in the hydrophobic layer of vesicle due to its hydrophobic nature. The ability of the synthesized scaffolds to encapsulate Nile Red was investigated by dialysis method. The dye loading content was calculated using Beer's law.

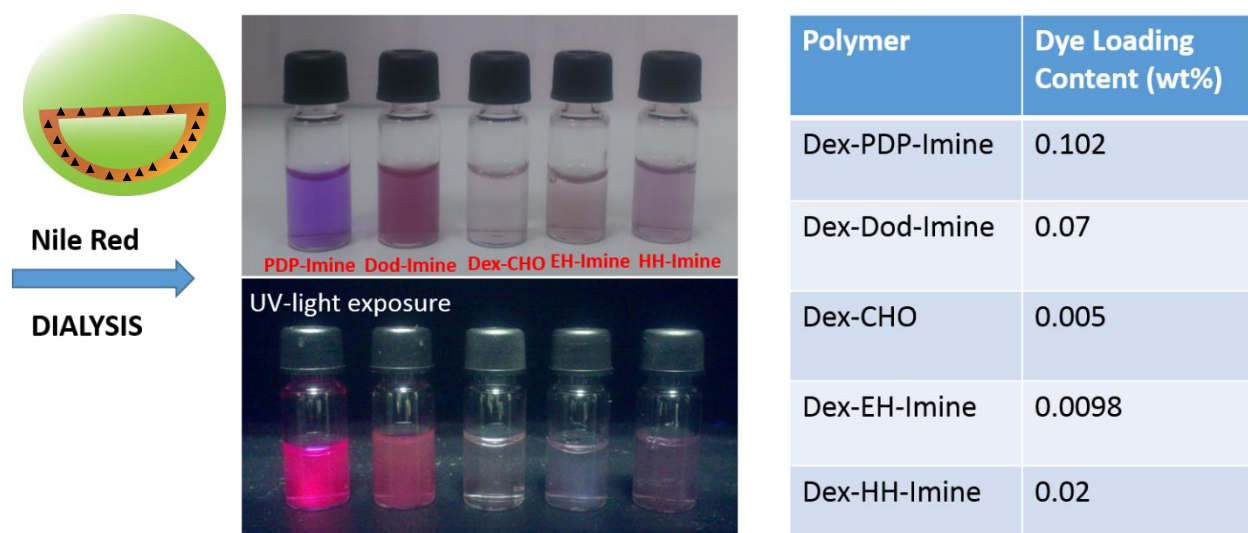


**Fig. 3.10** Nile Red encapsulated scaffolds under white light & upon photo excitation. Table.3. dye loading content of the encapsulated scaffolds.

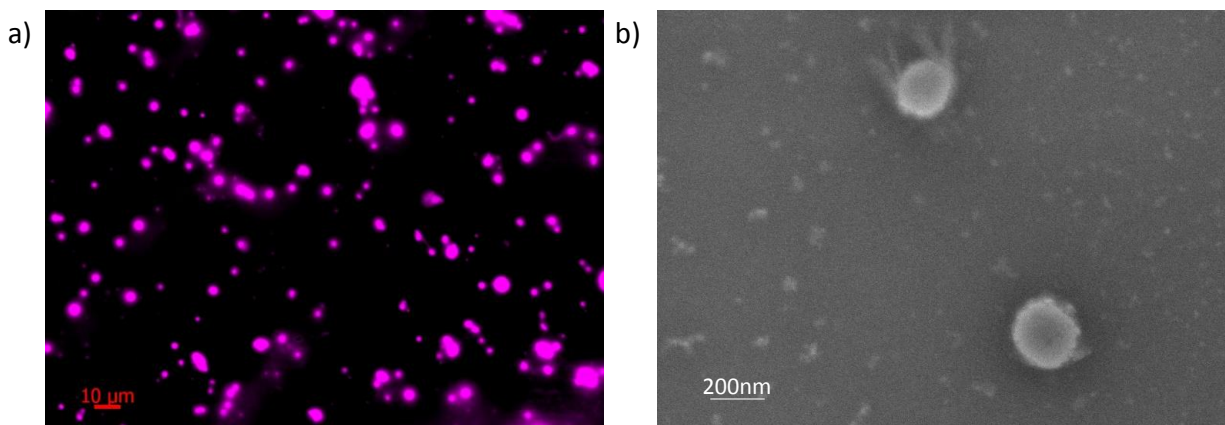


**Fig. 3.11** a) Fluorescence microscopy image and b) FE-SEM image of Nile red encapsulated Dex-PDP-IM.

As expected, the Dex-PDP-IM encapsulated the Nile Red dye effectively than the other scaffolds. Whereas Dex-Dod-IM also showed a weak encapsulation of the hydrophobic dye having DLC of 0.07 wt%. Out of these five scaffolds, Dex-PDP-IM showed the highest dye loading content owing to the formation of vesicular assembly. From FE-SEM images, it is evident that the vesicular morphology is retained even after the encapsulation of Nile red and fluorescence microscopy images confirm that the dye is exactly localized inside the vesicle (Fig 3.11).

### 3.3.3 Pyrene as hydrophobic dye

Another hydrophobic dye used as a probe to study about the hydrophobic region of vesicular assembly was pyrene. The ability of scaffolds to encapsulate the dye was calculated using the dialysis method and the results are shown in Fig.3. Only the Dex-PDP-IM scaffold showed the effective encapsulation of pyrene over the other scaffolds as expected. This was due to the fact that only Dex-PDP-IM self-assembles into vesicular assembly thus can encapsulate both hydrophobic as well as hydrophilic dye in it.

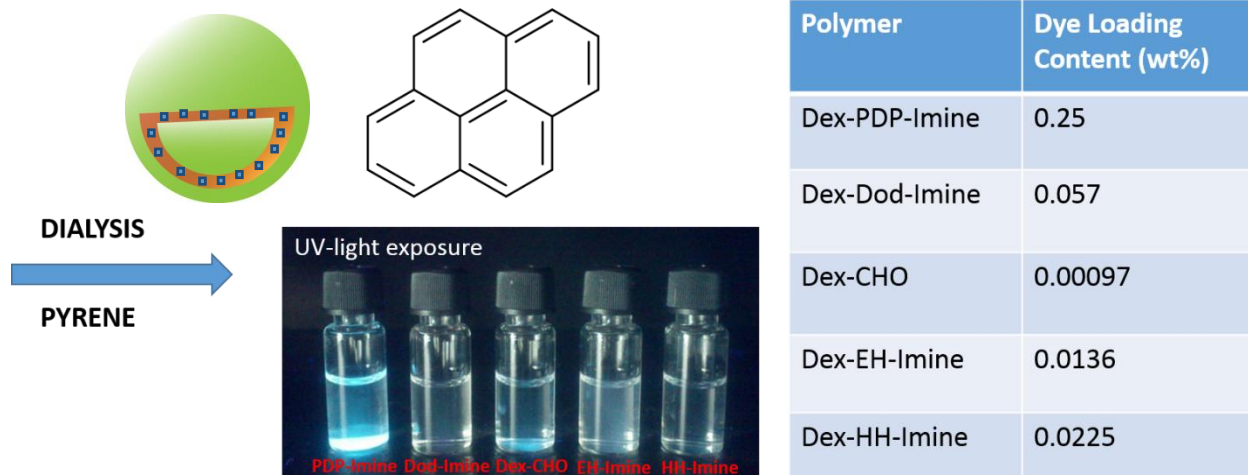


**Fig.3.12** Pyrene encapsulated scaffolds upon photo excitation. Table.3. dye loading contents of the scaffolds.

Furthermore, an attempt was made to encapsulate both pyrene and Rh B to the Dex-PDP-IM scaffold simultaneously. After dialysis for 24 hours, absorbance of the sample was measured using UV-Vis spectrophotometer. It showed both Rh B absorption maximum peak at 556 nm as well as pyrene's characteristic peak at 337 nm (Fig 3. 13).

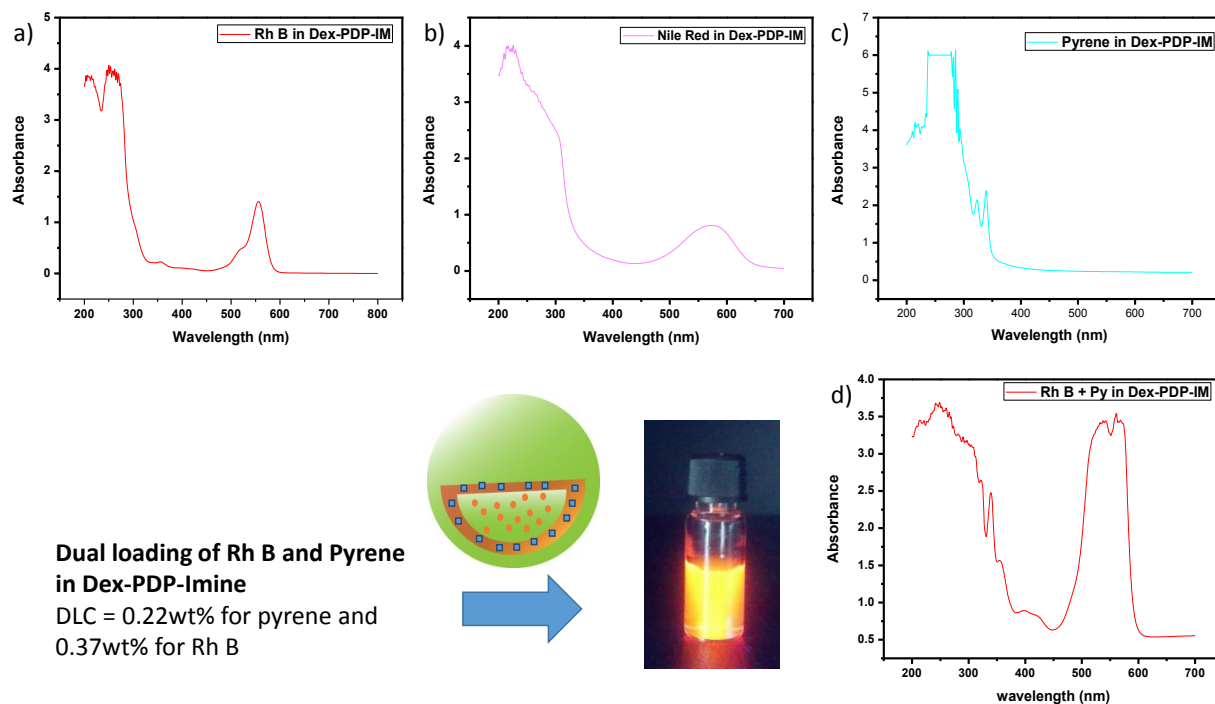


**Fig.3.13** Absorbance of Rh B (a) Nile red (b) and Pyrene (d) in Dex-PDP-IM. Dual dye loading of Rh B and pyrene in Dex-PDP-IM scaffold (d).

Further studies are under the way to check whether the dyes inside the vesicles are interacting with each other or not using FRET mechanism since there is spectral overlap between emission of pyrene and absorption of Rh B.

### IN VITRO RELEASE STUDIES

By modelling Rh B as a hydrophilic dye, the release kinetics for the scaffold Dex-PDP-IM at three different pH were performed i.e. pH = 7.4 (physiological pH), pH = 5.5 (endosomal pH) and pH = 2 (extreme acidic pH). Fig.3.14 shows the release characteristics of Rh B encapsulated Dex-PDP-IM at three different pH. The amount of Rh B encapsulated within the Dex-PDP-IM vesicles was found using Beer's law.

$DLC (\%) = (\text{weight of dye in vesicles} / \text{weight of dye loaded vesicles}) \times 100.$

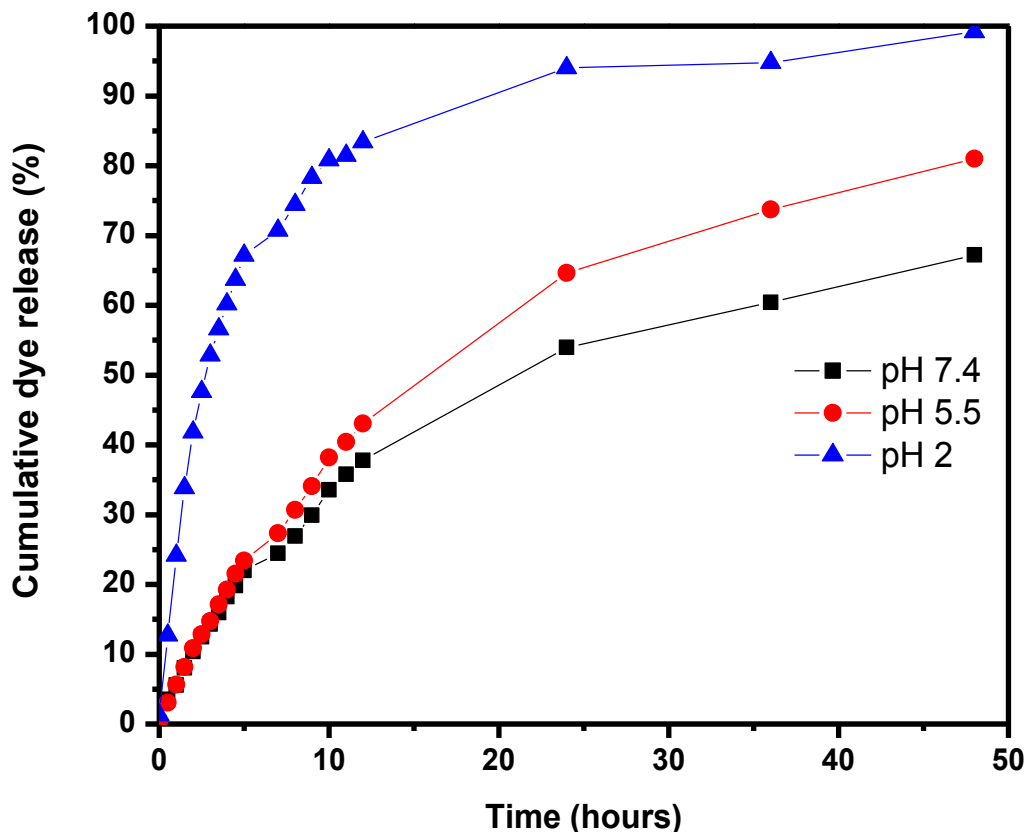


Fig.3.14 The release kinetics of Rh B encapsulated in Dex-PDP-IM at three different pH.

The encapsulation efficiency was calculated to be 0.46 wt. %. The Dex-PDP-IM is linked by imine bond between the hydrophobic and hydrophilic units. This imine linkage is acid labile, which can be cleaved under acidic conditions. At pH 7.4, it was found that 45-50% of the dye was retained in the scaffold. This implies that at physiological pH release of Rh B is due to natural leaching which happens due to constant perturbation in the form of stirring during dialysis. But at pH 5.5 and 2 release is due to the rupturing of vesicular membrane by cleaving the imine bond. At pH 5.5, around 80% of the dye gets released from the scaffold by cleaving the vesicular assembly. And at pH 2 extreme acidic condition almost 100% release of Rh B from Dex-PDP-IM was obtained. This is due to the fact that, in acidic conditions imine linkage breaks to corresponding amine and aldehyde and thereby disassembly of the vesicle happens results in the release of Rh B.

Further studies are underway to assure the release kinetics of anticancer drugs like camptothecin, doxorubicin independently into the Dex-PDP-IM scaffold. Moreover this scaffold will be employed for further cytotoxic studies (MTT assay).

## CONCLUSION

In this study, we have designed and synthesized dextran based pH responsive amphiphiles in order to ascertain the role of hydrophobic units in the self-assembly of nanoscaffolds. The hydrophobic units were carefully chosen for the study includes linear chain, branched chain and aromatic long chain etc. The synthetic approach includes, firstly grafting an aldehyde unit to the dextran backbone using DCC/DMAP coupling and then coupling this aldehyde bearing dextran (DS = 12%) with hydrophobic amine functionality using simple iminization reactions. The structure of the newly synthesized amphiphiles were confirmed using NMR and FT-IR. The self-assembled amphiphiles showed sizes ranging from 110-260nm depending on the hydrophobic unit. The self-assembly studies were done using FE-SEM and dynamic light scattering techniques. The loading capabilities of the scaffolds were investigated using hydrophobic as well as hydrophilic dyes like Nile red, pyrene and Rh B. Out of the synthesized pH responsive amphiphiles only Dex-PDP-IM could encapsulate both hydrophobic and hydrophilic dyes independently as well as simultaneously. So the further studies were carried out with this particular scaffold Dex-PDP-IM which showed nice vesicular self-assembly from microscopic techniques. The release kinetics was performed for Rh B loaded Dex-PDP-IM scaffold at three different pH and observed that there is ~50% intrinsic leaching at physiological pH, at endosomal pH (5.5) ~80% of the dye gets released and in extreme acidic condition (pH 2) almost 100% dye release occurs.

## REFERENCES:

- 1 Ramirez De Molina, A., Rodriguez-Gonzalez, A. & Lacal, J. C. Targeting new anticancer drugs within signalling pathways regulated by the Ras GTPase superfamily (Review). *International journal of oncology* **19**, 5-17 (2001).
- 2 Le Garrec, D. *et al.* Poly(N-vinylpyrrolidone)-block-poly(D,L-lactide) as a new polymeric solubilizer for hydrophobic anticancer drugs: in vitro and in vivo evaluation. *Journal of controlled release : official journal of the Controlled Release Society* **99**, 83-101, doi:10.1016/j.jconrel.2004.06.018 (2004).
- 3 Shen, Y. *et al.* Prodrugs forming high drug loading multifunctional nanocapsules for intracellular cancer drug delivery. *Journal of the American Chemical Society* **132**, 4259-4265, doi:10.1021/ja909475m (2010).
- 4 Tiwari, G. *et al.* Drug delivery systems: An updated review. *International journal of pharmaceutical investigation* **2**, 2-11, doi:10.4103/2230-973X.96920 (2012).
- 5 Uhrich, K. E., Cannizzaro, S. M., Langer, R. S. & Shakesheff, K. M. Polymeric systems for controlled drug release. *Chemical reviews* **99**, 3181-3198 (1999).
- 6 Farokhzad, O. C. & Langer, R. Impact of nanotechnology on drug delivery. *ACS nano* **3**, 16-20, doi:10.1021/nn900002m (2009).
- 7 Ambade, A. V., Savariar, E. N. & Thayumanavan, S. Dendrimeric micelles for controlled drug release and targeted delivery. *Molecular pharmaceutics* **2**, 264-272, doi:10.1021/mp050020d (2005).
- 8 Hatefi, A. & Amsden, B. Biodegradable injectable in situ forming drug delivery systems. *Journal of controlled release : official journal of the Controlled Release Society* **80**, 9-28 (2002).
- 9 Torchilin, V. P. Structure and design of polymeric surfactant-based drug delivery systems. *Journal of controlled release : official journal of the Controlled Release Society* **73**, 137-172 (2001).
- 10 Matsumura, Y. & Maeda, H. A new concept for macromolecular therapeutics in cancer chemotherapy: mechanism of tumorotropic accumulation of proteins and the antitumor agent smancs. *Cancer research* **46**, 6387-6392 (1986).
- 11 Fang, J., Nakamura, H. & Maeda, H. The EPR effect: Unique features of tumor blood vessels for drug delivery, factors involved, and limitations and augmentation of the effect. *Advanced drug delivery reviews* **63**, 136-151, doi:10.1016/j.addr.2010.04.009 (2011).
- 12 Fang, J., Sawa, T. & Maeda, H. Factors and mechanism of "EPR" effect and the enhanced antitumor effects of macromolecular drugs including SMANCS. *Advances in experimental medicine and biology* **519**, 29-49, doi:10.1007/0-306-47932-X\_2 (2003).
- 13 Maeda, H. SMANCS and polymer-conjugated macromolecular drugs: advantages in cancer chemotherapy. *Advanced drug delivery reviews* **46**, 169-185 (2001).
- 14 Maeda, H., Bharate, G. Y. & Daruwalla, J. Polymeric drugs for efficient tumor-targeted drug delivery based on EPR-effect. *European journal of pharmaceuticals and biopharmaceutics : official journal of Arbeitsgemeinschaft fur Pharmazeutische Verfahrenstechnik e.V* **71**, 409-419, doi:10.1016/j.ejpb.2008.11.010 (2009).
- 15 Bae, Y. H., Vernon, B., Han, C. K. & Kim, S. W. Extracellular matrix for a rechargeable cell delivery system. *Journal of controlled release : official journal of the Controlled Release Society* **53**, 249-258 (1998).
- 16 Jeong, B., Bae, Y. H., Lee, D. S. & Kim, S. W. Biodegradable block copolymers as injectable drug-delivery systems. *Nature* **388**, 860-862, doi:10.1038/42218 (1997).
- 17 Baldwin, A. D. & Kiick, K. L. Polysaccharide-modified synthetic polymeric biomaterials. *Biopolymers* **94**, 128-140, doi:10.1002/bip.21334 (2010).

- 18 Sinha, V. R. & Kumria, R. Polysaccharides in colon-specific drug delivery. *International journal of pharmaceutics* **224**, 19-38 (2001).
- 19 Mizrahy, S. & Peer, D. Polysaccharides as building blocks for nanotherapeutics. *Chemical Society reviews* **41**, 2623-2640, doi:10.1039/c1cs15239d (2012).
- 20 Houga, C. *et al.* Micelles and polymersomes obtained by self-assembly of dextran and polystyrene based block copolymers. *Biomacromolecules* **10**, 32-40, doi:10.1021/bm800778n (2009).
- 21 Li, Y.-L. *et al.* Reversibly Stabilized Multifunctional Dextran Nanoparticles Efficiently Deliver Doxorubicin into the Nuclei of Cancer Cells. *Angewandte Chemie International Edition* **48**, 9914-9918, doi:10.1002/anie.200904260 (2009).
- 22 Pramod, P. S., Takamura, K., Chaphekar, S., Balasubramanian, N. & Jayakannan, M. Dextran vesicular carriers for dual encapsulation of hydrophilic and hydrophobic molecules and delivery into cells. *Biomacromolecules* **13**, 3627-3640, doi:10.1021/bm301583s (2012).
- 23 Pramod, P. S., Shah, R., Chaphekar, S., Balasubramanian, N. & Jayakannan, M. Polysaccharide nano-vesicular multidrug carriers for synergistic killing of cancer cells. *Nanoscale* **6**, 11841-11855, doi:10.1039/c4nr03514c (2014).
- 24 Torchilin, V. Multifunctional and stimuli-sensitive pharmaceutical nanocarriers. *European journal of pharmaceutics and biopharmaceutics : official journal of Arbeitsgemeinschaft fur Pharmazeutische Verfahrenstechnik e.V* **71**, 431-444, doi:10.1016/j.ejpb.2008.09.026 (2009).
- 25 Vander Heiden, M. G. Targeting cancer metabolism: a therapeutic window opens. *Nature reviews. Drug discovery* **10**, 671-684, doi:10.1038/nrd3504 (2011).
- 26 Zhu, L. & Torchilin, V. P. Stimulus-responsive nanopreparations for tumor targeting. *Integrative biology : quantitative biosciences from nano to macro* **5**, 96-107, doi:10.1039/c2ib20135f (2013).
- 27 Bajpai, A. K., Shukla, S. K., Bhanu, S. & Kankane, S. Responsive polymers in controlled drug delivery. *Progress in Polymer Science* **33**, 1088-1118, doi:<http://dx.doi.org/10.1016/j.progpolymsci.2008.07.005> (2008).
- 28 Helmlinger, G., Sckell, A., Dellian, M., Forbes, N. S. & Jain, R. K. Acid production in glycolysis-impaired tumors provides new insights into tumor metabolism. *Clinical cancer research : an official journal of the American Association for Cancer Research* **8**, 1284-1291 (2002).
- 29 Lee, E. S., Shin, H. J., Na, K. & Bae, Y. H. Poly(L-histidine)-PEG block copolymer micelles and pH-induced destabilization. *Journal of controlled release : official journal of the Controlled Release Society* **90**, 363-374 (2003).
- 30 Guo, X. & Szoka, F. C., Jr. Steric stabilization of fusogenic liposomes by a low-pH sensitive PEG--diortho ester--lipid conjugate. *Bioconjugate chemistry* **12**, 291-300 (2001).
- 31 Gao, W., Chan, J. M. & Farokhzad, O. C. pH-Responsive nanoparticles for drug delivery. *Molecular pharmaceutics* **7**, 1913-1920, doi:10.1021/mp100253e (2010).
- 32 Pramod, P. S., Shah, R. & Jayakannan, M. Dual stimuli polysaccharide nanovesicles for conjugated and physically loaded doxorubicin delivery in breast cancer cells. *Nanoscale*, doi:10.1039/C5NR00799B (2015).